TECHNICAL MANUAL

DESIGN OF STRUCTURES TO RESIST THE EFFECTS OF ATOMIC WEAPONS

ARCHES AND DOMES

This is a reprint of former EM 1110–345–420, 15 January 1960. Redesignated TM 5–856–8 by DA Cir 310–28, 17 March 1965.

HEADQUARTERS, DEPARTMENT OF THE ARMY

JANUARY 1960

HEADQUARTERS
DEPARTMENT OF THE ARMY
WASHINGTON, D.C., *15 January 1960*

TM 5–856–8 is published for the use of all concerned.

By Order of the Secretary of the Army:

LYMAN L. LEMNITZER
General, United States Army
Chief of Staff

OFFICIAL:
R. V. LEE
Major General, United States Army
The Adjutant General

☆ U.S. GOVERNMENT PRINTING OFFICE: 1971—480–803/3106A

ENGINEERING AND DESIGN

DESIGN OF STRUCTURES TO RESIST THE EFFECTS OF ATOMIC WEAPONS

ARCHES AND DOMES

TABLE OF CONTENTS

ENGINEERING AND DESIGN

DESIGN OF STRUCTURES TO RESIST THE EFFECTS OF ATOMIC WEAPONS
ARCHES AND DOMES

INTRODUCTION

10-01 PURPOSE AND SCOPE. This manual is one in a series issued for the guidance of engineers engaged in the design of permanent-type military structures required to resist the effects of atomic weapons. It is applicable to all Corps of Engineers activities and installations responsible for the design of military construction.

The material is based on the results of full-scale atomic tests and analytical studies. The problem of designing structures to resist the effects of atomic weapons is new and the methods of solution are still in the development stage. Continuing studies are in progress and supplemental material will be published as it is developed.

The methods and procedures were developed through the collaboration of many consultants and specialists. Much of the basic analytical work was done by the engineering firm of Ammann and Whitney, New York City, under contract with the Chief of Engineers. The Massachusetts Institute of Technology was responsible, under another contract with the Chief of Engineers, for the compilation of material and for the further study and development of design methods and procedures.

It is requested that any errors and deficiencies noted and any suggestions for improvement be transmitted to the Office of the Chief of Engineers, Department of the Army, Attention: ENGEB.

10-02 REFERENCES. Manuals - Corps of Engineers - Engineering and Design, containing interrelated subject matter, are listed as follows:

DESIGN OF STRUCTURES TO RESIST THE EFFECTS
OF ATOMIC WEAPONS

EM 1110-345-413 Weapons Effects Data
EM 1110-345-414 Strength of Materials and Structural Elements
EM 1110-345-415 Principles of Dynamic Analysis and Design

EM 1110-345-416 Structural Elements Subjected to Dynamic Loads
EM 1110-345-417 Single-Story Frame Buildings
EM 1110-345-418 Multi-Story Frame Buildings
EM 1110-345-419 Shear Wall Structures
EM 1110-345-420 Arches and Domes
EM 1110-345-421 Buried and Semiburied Structures

a. References to Material in Other Manuals of This Series. In the text of this manual references are made to paragraphs, figures, equations, and tables in the other manuals of this series in accordance with the number designations as they appear in these manuals. The first part of the designation which precedes either a dash, or a decimal point, identifies a particular manual in the series as shown in the table following.

EM	paragraph	figure	equation	table
1110-345-413	3-	3.	(3.)	3.
1110-345-414	4-	4.	(4.)	4.
1110-345-415	5-	5.	(5.)	5.
1110-345-416	6-	6.	(6.)	6.
1110-345-417	7-	7.	(7.)	7.
1110-345-418	8-	8.	(8.)	8.
1110-345-419	9-	9.	(9.)	9.
1110-345-420	10-	10.	(10.)	10.
1110-345-421	11-	11.	(11.)	11.

b. Bibliography. A bibliography is given at the end of the text. Items in the bibliography are referenced in the text by numbers inclosed in brackets.

c. List of Symbols. Definitions of the symbols used throughout this manual series are given in a list following the table of contents in EM 1110-345-413 through EM 1110-345-416.

10-03 RESCISSIONS. (Draft) EM 1110-345-420 (Part XXIII - The Design of Structures to Resist the Effects of Atomic Weapons, Chapter 10 - Arches and Domes).

10-04 PRINCIPLES AND PROCEDURES. This manual is concerned with the resistance of arch and dome structures to air-blast loading. Because the structural analysis of arches and domes is inherently complex, exact design procedures are impractical and the procedures employed in this manual are, for this reason, of a more approximate nature than design procedures employed for other structures.

Certain similarities exist in the design procedures for arches and)mes, and for this reason, both procedures are presented in this manual.

Arch and dome structures can be lightly covered with earth conform-ıg in shape generally to the outline of the structure. In such cases the ırth cover will serve to increase the effective mass of the structure and lso to increase the rise time of the applied dynamic loads. Deep burial ? the structure is not considered in this manual, and for their coverage ıe reader is referred to EM 1110-345-421, Buried and Semiburied Struc-ıres, and reference [15].

ARCHES

)-05 TYPES OF STRUCTURES CONSIDERED. The method presented is illustrated r the design of an arch of semicircular cross section, but the method is)t restricted to this type of structure. The method may be applied to ıose structures whose cross section is an arc of a circle or can be ap-:oximated by an arc of a circle. Only structures with resistant covering ıich cannot fail or be blown off by the blast wave are considered. Such a ;ructure might be a barrel arch of reinforced concrete, or it may be con-;ructed of steel or concrete ribs supporting a monolithic concrete slab)vering or concrete panels.

In general, the design of the covering of the arch ribs is governed r the same principles that apply to panels in walls or roofs of other ;ructures. The applicable methods of analysis are covered in other man-ıls of this series; this manual is concerned only with the behavior of ıe arched or domed elements.

The presence of end walls or intermediate walls or stiffening ribs ı a long structure will supply rigidity to an arch and increase its re-.stance to side loads. This increased rigidity will manifest itself when ıe spacing of these stiffeners is fairly small. Considering an arched ;ructure of the thin shell type with no intermediate stiffeners, the pres-ıce of the end walls influences the structural response of the arch when ıe spacing of these end walls is equal to or less than $0.75\sqrt{Rt}$, where R ; the radius of the arch and t is its thickness. If intermediate

diaphragms or stiffeners are added, their effectiveness only becomes apparent when their spacing is less than $1.50\sqrt{Rt}$. See reference [9]. This latter spacing is based on the assumption that complete fixity exists at the junction of the stiffener and the arch. For an arch with a radius of 30 ft and a thickness of 1 ft, the spacing of these stiffeners must be less than approximately 8 ft to affect the response of the arched elements to the applied dynamic loads.

In most instances this spacing will be less than is economically feasible. In any event, disregarding the effect of the end walls and intermediate stiffeners on the arch response will be conservative, and for this reason is not considered.

10-06 TYPES OF LOADING. a. General Concepts. The basic ideas regarding blast loading of structures are presented in EM 1110-345-413, where methods are given for determining the local forces due to the incident overpressure wave and the high velocity winds associated with it. Certain aspects of the loading that have a bearing on the resistance of the structure will be reviewed here.

b. Blast Wave Approaching Along the Arch Axis. When a blast wave approaches the structure from a direction perpendicular to the end walls, and the end walls are resistant to the blast, the structure is enveloped in essentially a uniform external force traveling axially along the arch. The magnitude of this load is the free air overpressure and is illustrated in figure 10.1. Considering a strip of differential width measured along the arch axis, the compressive loading would be instantaneously applied, that is, the time for the load to reach its maximum intensity would be zero. The

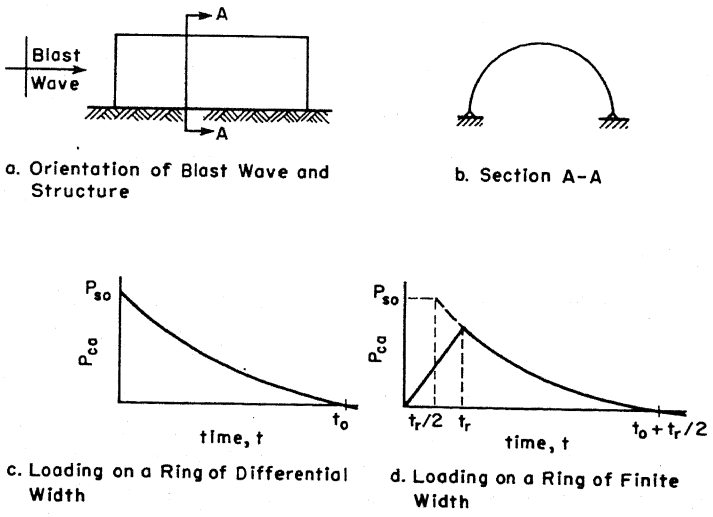

Figure 10.1. Loading on a circular arch element for axially approaching blast wave

expression for this compressive loading as a function of time is:

$$P_{ca} = P_{so} (1 - t/t_o) e^{-t/t_o} \qquad (10.1)$$

where

t = time measured from the instant the blast wave reaches the strip of differential width being considered

t_o = the duration of the positive phase of the incident blast wave

P_{ca} = the uniform compressive force applied radially

P_{so} = the maximum incident overpressure

The variation of this loading as a function of time is illustrated in figure 10.1c.

For an element of finite width w the average compressive load on the element would reach its maximum intensity at the instant that the blast wave had just passed over the entire width of the strip. Its magnitude would be the value of the incident overpressure existing at the center of the strip. This assumes a linear variation of overpressure over the distance w ; an assumption which is valid if the time required for the blast wave to traverse this distance is small compared to the duration of the blast wave (less than about $0.1\ t_o$). The time to reach maximum compressive loading is

$$t_r = w/U_o \qquad (10.2)$$

and the intensity of this compressive loading after time t_r is

$$P_{ca} = P_{so} \left(1 - \frac{t - 1/2\ t_r}{t_o}\right) e^{-(t - 1/2\ t_r)/t_o} \qquad (10.3)$$

where U_o is the shock front velocity. The variation of this loading is illustrated in figure 10.1d.

A detailed discussion of the structural response under this type of loading is given later in this manual.

c. Blast Wave Approaching Normal to the Arch Axis. When the blast wave approaches a resistant structure from the side, the pressures on the

"windward" and "leeward" sides of the arch are different, each varying with time. Because of the higher reflected pressures on the more nearly vertical faces near the support, the pressures on the near or windward side become quite large almost immediately. The magnitude of the pressure on the leeward or far side is relatively low until the blast wave traveling over the arch strikes the ground on the far side of the structure. However, the overpressures on this side of the arch are never greater than the incident overpressure. Eventually, after a time equal to about five or six times the time required for the shock wave to travel over the arch, the pressures are fairly equal over the entire surface, and the structure would act as though it were in a region of uniform external overpressure were it not for the motions imparted to it in the earlier stages of loading by the incident blast wave.

Because of the unbalanced loading at the beginning, the arch is subjected to lateral forces causing lateral movement of the crown, an inward deflection on the windward side and an outward deflection on the leeward side as illustrated by the dashed lines of figure 10.2. These distortions are accompanied by an axial shortening and bending of the arch. Fortunately, the two components of distortion can be considered separately, and the response of the structure can be determined by convenient approximations. The methods for doing this are described in subsequent paragraphs.

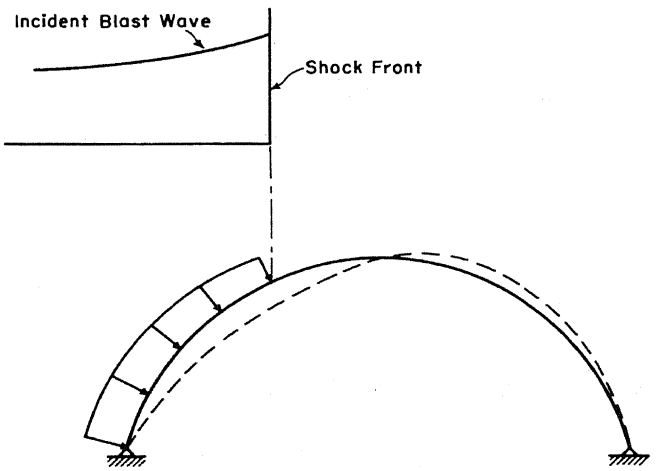

Figure 10.2. Deflected shape of arch during early stages of blast loading (blast wave normal to arch axis)

d. Determination of Component Loadings for Blast Wave Normal to the Arch Axis. Because of the nature of the resistance of the structure, it is desirable to separate the actual loading into components: (1) symmetrical or "compression mode" loading, and (2) antisymmetrical or "deflection mode" loading. For a symmetrical elastic structure there are a series of modal

ıdings and of corresponding modal responses of each of the two components. ; determination of these modal loadings is fairly complex, and depends on ; shape of the arch axis, its various values of linear and flexural ri- .ities, and the variations in section from springing point to crown. rever, these modes are not separable in the inelastic range. A good ap- ximation to the response of the structure can be obtained by a more mentary consideration, assuming that only one of the two modes is im- tant in the deformation associated with each loading component.

Because of the complexities of the problem, and primarily to achieve ethod that is simple, the modal loadings are determined herein by a hod of averaging the forces on each half of the arch. This assumes that re is no variation of overpressure over the windward side and leeward e of the arch and that the overpressure at any time t can be expressed an average value for the windward side and another average value for the ward side. This is not the most accurate method which can be devised the lack of precise knowledge of the actual blast loadings and the uctural properties makes the use of more precise methods somewhat ques- nable. The recommended procedure is as follows:

Let the overpressure normal to the arch barrel at any point and at time be designated by $P(t)$ On the basis of the discussion in the vious paragraph this varying load can be replaced by two average load- s, one for the windward or near side of the arch, and another for the ward or far side of the arch. Let these two average values used to re- ce the actual load distribution over the arch be designated by P_n and , respectively. This average loading system can now be replaced by an ivalent set of symmetrical and antisymmetrical loadings. These loadings designated as the compression mode loading P_c and the deflection mode ding P_d, respectively, and are defined as follows:

$$\left.\begin{aligned} P_c &= 0.5\,(P_n + P_f) \\ P_d &= 0.5\,(P_n - P_f) \end{aligned}\right\} \qquad (10.4)$$

As an illustration of the application of the preceding development, sider a semicircular arch loaded as shown in figure 10.3a. This actual

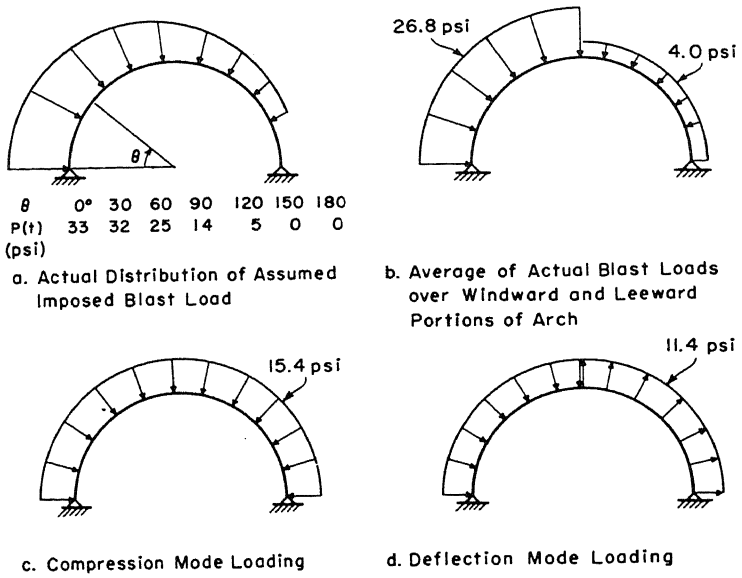

Figure 10.3. Computation of modal loadings from imposed blast loadings

assumed loading is now replaced by a system consisting of two intensities, nonvarying over the windward and leeward sides of the arch. The intensities are the average values of the actual loadings over these two halves of the arch. Applying the trapezoidal integration formula to figure 10.3a we have

$$\text{for the near side, } P_n = \frac{1}{3}\left(\frac{33}{2} + 32 + 25 + \frac{14}{2}\right) = 26.8 \text{ psi}$$

$$\text{for the far side, } P_f = \frac{1}{3}\left(\frac{14}{2} + 5 + 0 + \frac{0}{2}\right) = 4.0 \text{ psi}$$

These loadings are illustrated in figure 10.3b.

Equation (10.4) is now applied to this averaged loading system to obtain the two modal loadings, yielding

$$P_c = 0.5\ (26.8 + 4.0) = 15.4 \text{ psi}$$
$$P_d = 0.5\ (26.8 - 4.0) = 11.4 \text{ psi}$$

These modal loadings are illustrated in figures 10.3c and d. Note that the superposition of the compression mode loading of figure 10.3c on the deflection mode loading of figure 10.3d yields the averaged loading of b which is assumed equivalent to the actual loading of part a of this same figure.

The pressure-time relations for any point on the arch can be deter-ined by the procedures given in paragraph 3-17 of EM 1110-345-413. The ore load points considered on the arch, the more accurate will be the alues of P_c and P_d. About seven to nine points equally spaced around ie arch should be sufficient.

e. Approximate Values of Modal Loadings for Blast Wave Normal to ie Arch Axis. A simplified approximation to the loading obtained by the ethods given in paragraph 3-17 is given in this section. These approxi-ite loadings can be used for preliminary designs or where greater accuracy s not considered to be worth the extra work involved. These approximate adings give conservative esults and although they y, in some cases, yield rger values for the im-lse, they will give only ightly greater values of e required resistance of e arch element.

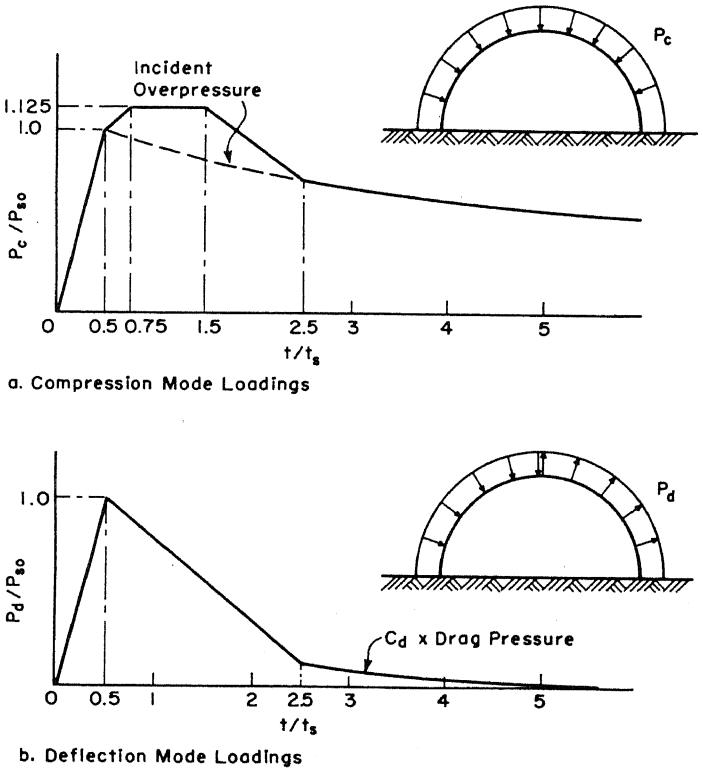

Figure 10.4. Approximate modal loadings

From estimates of the ading obtained through the e of the methods outlined paragraph 3-17 which are sed on shock tube data and udies of test data from eration GREENHOUSE it ap-ars that the modal loadings n be represented adequately approximate curves as own in figure 10.4. The time scale is given in terms of the transit time , the time required for the shock front to pass over the span of the ch. For convenience in determining the magnitude of the compression mode adings at times in excess of $2.5t_s$, the incident overpressure curve as a nction of time is plotted with its origin at time $t_s/2$, the time the ock front reaches the crown of the arch.

Both components are equal for values of t less than the time required for the shock front to reach the crown of the arch. The deflection mode overpressure drops linearly from a maximum value of P_{so} to the drag pressure produced by the incident overpressure existing at time $t = 2.5\ t_s$, multiplied by the drag coefficient C_d. Rough calculations indicate a value of $C_d = 0.2$ for values of Reynolds number greater than 5×10^5 and a value of $C_d = 0.6$ for values of Reynolds number less than 5×10^5. The drag coefficient C_d in this section is equal to one-half the average of the local drag coefficients C_D on the windward side minus one-half the average of the local drag coefficients on the leeward side. The variation of local drag coefficients with position on the arch is illustrated in paragraph 3-17.

The drag pressure produced by any value of the incident overpressure can be calculated reasonably closely by the approximate relation

$$\text{drag pressure} = 0.022\ P_s^{\,2} \tag{10.5}$$

The Reynolds number associated with this incident overpressure can be approximated by the relation

$$R_e = 60{,}000\ P_s D\ (17.1 + P_s)^{1/2} \tag{10.6}$$

where, referring to figure 10.4, P_s is the incident overpressure in psi at time $t - t_s/2$ and D is the diameter of the arch in feet.

It is possible for the deflection mode overpressure to become negative when the average loading on the leeward side of the arch exceeds that on the windward side. However, the negative values are not usually large and do not last very long under ordinary circumstances.

f. Loading Produced by the Blast Wave Approaching at an Angle to the Arch Axis. When the blast wave approaches the structure at an angle, the determination of the forces imposed on the arch is difficult. Since the direction of loading which produces critical response is either normal to the arch axis, or parallel to it, these are the only two conditions considered in this manual.

10-07 STRUCTURAL RESISTANCE. a. Response to Compression Mode Loading. The response of the structure to either of the modal loadings depends upon the characteristics of the structure. In order to determine the response, estimates must be made of the natural frequencies of vibration of the structure in the two modes, and of the yield resistance as well as the ductility ratio or ratio of maximum allowable deflection to the yield deflection.

For convenience in making such calculations, an idealized elasto-plastic resistance is assumed, and the frequency is determined for a structure having a stiffness corresponding to that associated with the yield resistance divided by the yield deflection. Also, in a fixed-end structure the resistance corresponds to that after plastic hinges have formed at several points, including the incipient final plastic hinge which leads to collapse.

In the compression mode, the arch is very stiff and the period is consequently very short.

For a circular arch with pinned ends and of constant cross section the lowest natural frequency is one for which the arch vibrates in the shape shown by the dashed curve of figure 10.5. The natural period of vibration, in seconds, for this mode of vibration is given by the relation [2, 7]

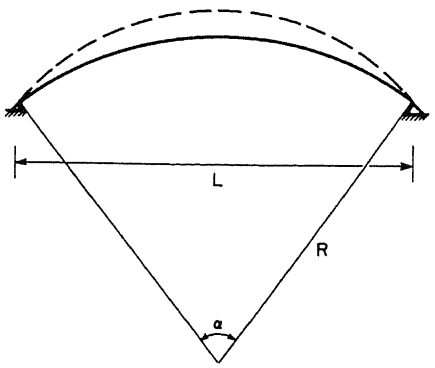

Figure 10.5. Vibrational shape associated with the lowest natural frequency of a two-hinged arch in the compression mode

$$T_n = \frac{2\pi L^2}{C_1}\sqrt{\frac{m}{EI}} \qquad (10.7)$$

where

L = the span of the arch in in.

E = the modulus of elasticity in lb/in.^{2}

I = the moment of inertia of the arch cross section in in.^{4}

m = the mass per in. of circumferential length of arch in lb-sec^2/in.^{2}

$$C_1 = 4 \sin^2 \frac{\alpha}{2} \sqrt{0.820 \left(\frac{R}{k}\right)^2 + \left(\frac{\pi^2}{\alpha^2} - 1\right)^2} \qquad (10.8)$$

where R is the radius of the arch in in. and k is the radius of gyration of the cross section in in.

For a circular arch with fixed ends and of constant cross section, the lowest natural frequency is one for which the arch vibrates in the shape shown by the dotted curve of figure 10.6. In this case the period is given by [2, 7]

$$T_n = 2\pi \frac{L^2}{C_2} \sqrt{\frac{m}{EI}} \qquad (10.9)$$

where

$$C_2 = 4 \sin^2 \frac{\alpha}{2} \sqrt{\frac{2}{3} \left(\frac{R}{k}\right)^2 + \left(\frac{\pi^2}{\alpha^2} - 1\right)^2} \qquad (10.10)$$

and where k is the radius of gyration of the cross section of the arch.

It is fairly evident from a study of these relations that the period of vibration for an arch in the compression mode is relatively short. For example, consider the arch illustrated in figure 10.7. Approximate values for this arch are as follows:

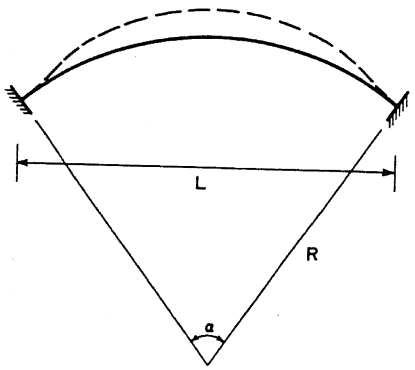

Figure 10.6. Vibrational shape associated with lowest natural frequency of a fixed-end arch in the compression mode

$I_a = 6000$ in.^{4}
$m = 0.0565$ lb-sec^2/in.
$A_a = 195$ in.^{2}

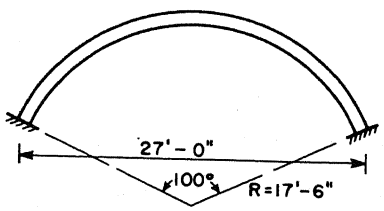

a. Elevation of Arch

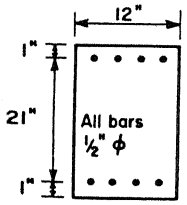

b. Typical Cross Section of Arch

Figure 10.7. Sample arch

$k = 5.55$ in.

$L = 324$ in.

$e = 3 \times 10^6$ lb/in.^{2}

$C_2 = 74.5$ from equation (10.10)

$R = 210$ in.

For these data, from equation (10.9)

$$T_n = 2\pi \frac{L^2}{C_2} \sqrt{\frac{m}{EI}} = 0.015 \text{ sec}$$

Considering elastic behavior, the significance of this short period combined with the compression mode loading is that the stresses produced are essentially those which would be produced by this same load applied statically. This is due to the fact that as the rise time of the imposed compression mode loading approaches the natural period of the structure the dynamic load factor approaches unity.

Furthermore, it would not be desirable to permit the loading in the compression mode to exceed the yield resistance of the structure. That is, in reinforced concrete, the stresses produced by the compression mode loading should be less than the dynamic cylinder strength of the concrete and less than the dynamic yield strength of the steel. The applied compression mode loading is carried primarily by direct stress in the arch. Since the variation of axial stress is approximately uniform over finite lengths of the arch, allowing the stresses to reach their dynamic yield values will result in the formation of plastic hinges which extend over a finite length of the arch, rather than at localized points. This will result in a "softening" of the arch and a correspondingly large increase in deflections which is not desirable.

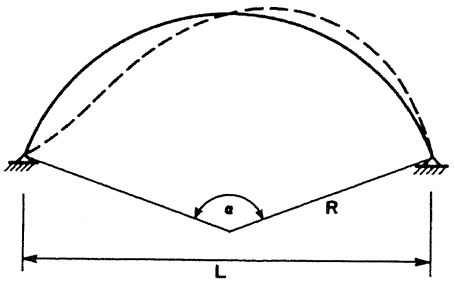

Figure 10.8. Vibrational shape associated with lowest natural frequency of a two-hinged arch in the deflection mode

b. Response to Deflection Mode Loading. In the deflection mode the structure is relatively flexible as compared to its behavior in the compression mode.

The dotted curve of figure 10.8 shows

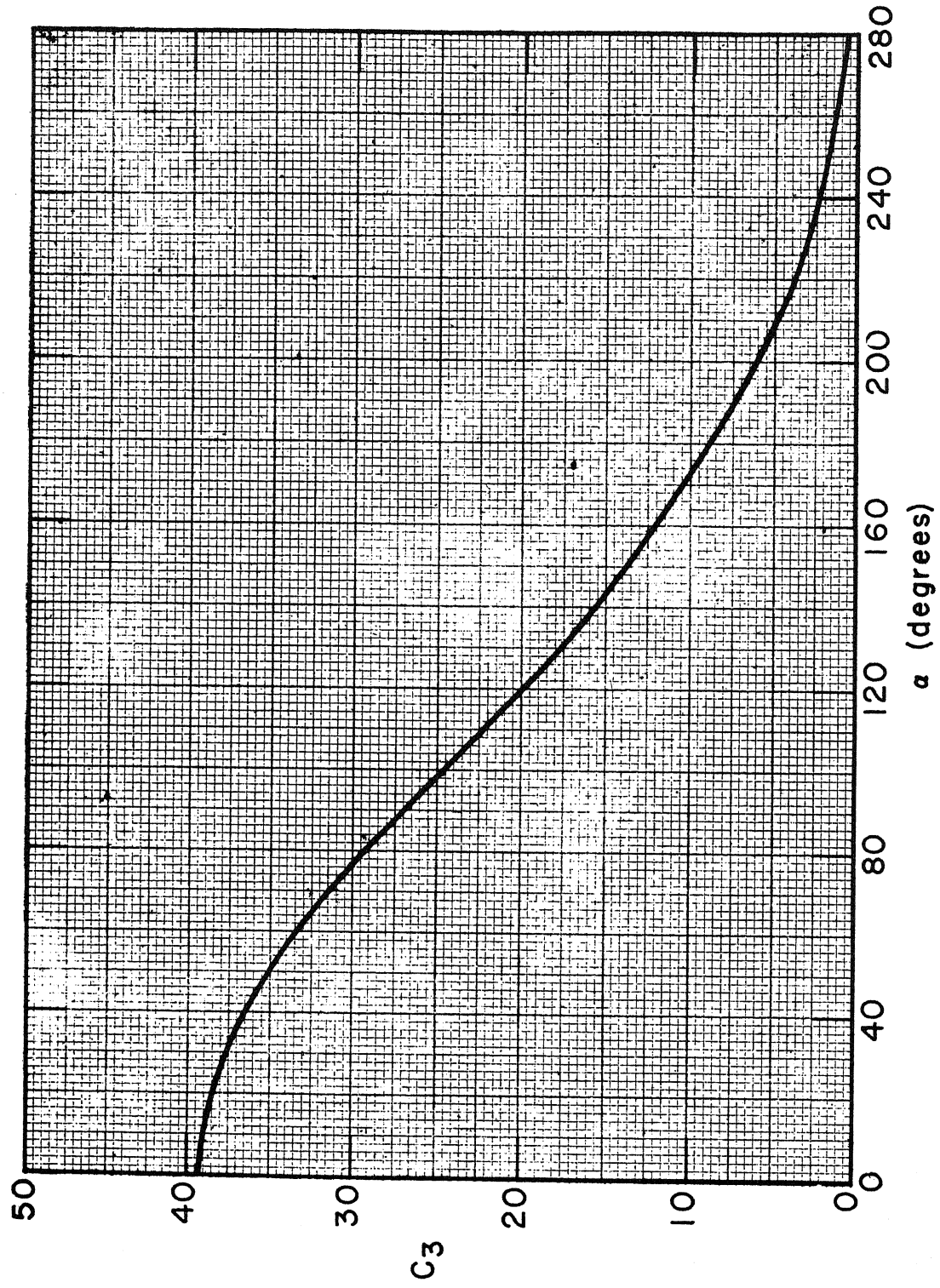

Figure 10.9. Vibration parameter C_3 as a function of the central angle α for a two-hinged arch in the deflection mode

the shape of the natural period of vibration for a circular arch with pinned ends and of constant cross section. The natural period of vibration is given by the relation [2, 7]

$$T_{nd} = \frac{2\pi L^2}{C_3}\sqrt{\frac{m}{EI}} \qquad (10.11)$$

where C_3 is plotted in figure 10.9.

For a circular arch with fixed ends, and of constant cross section the natural period of vibration is one for which the arch vibrates in the shape shown by the dotted curve of figure 10.10. The natural period of vibration is given by the relation [2, 7]

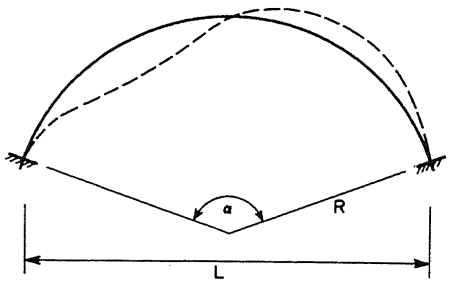

Figure 10.10. Vibrational shape associated with lowest natural frequency of a fixed-end arch in the deflection mode

$$T_{nd} = \frac{2\pi L^2}{C_4}\sqrt{\frac{m}{EI}} \qquad (10.12)$$

where C_4 is plotted in figure 10.11.

Equations (10.11) and (10.12) are based on the assumption that the primary behavior in this mode is in flexure with a consequent neglect of axial deformation. Except for very flat arches, α less than about 50°, the accuracy of these relations is good.

Because of the long natural period of vibration and the correspondingly short duration of the deflection mode loading, the response of the structure can be estimated as if it were loaded by an equivalent rectangular pulse of the same area as that under the deflection mode loading curve. The impulse due to the continued drag loading is very small compared with that of the initial unbalanced pressure loading and can be either neglected entirely or an initial impulse can be used which is large enough to account for the entire area under the curve of deflection mode loading as given in figure 10.4 or as computed by the procedure given in paragraph 10-06c. This latter procedure will overestimate the effect of the continued drag loading.

For the triangular shaped deflection mode loading of figure 10.4, a

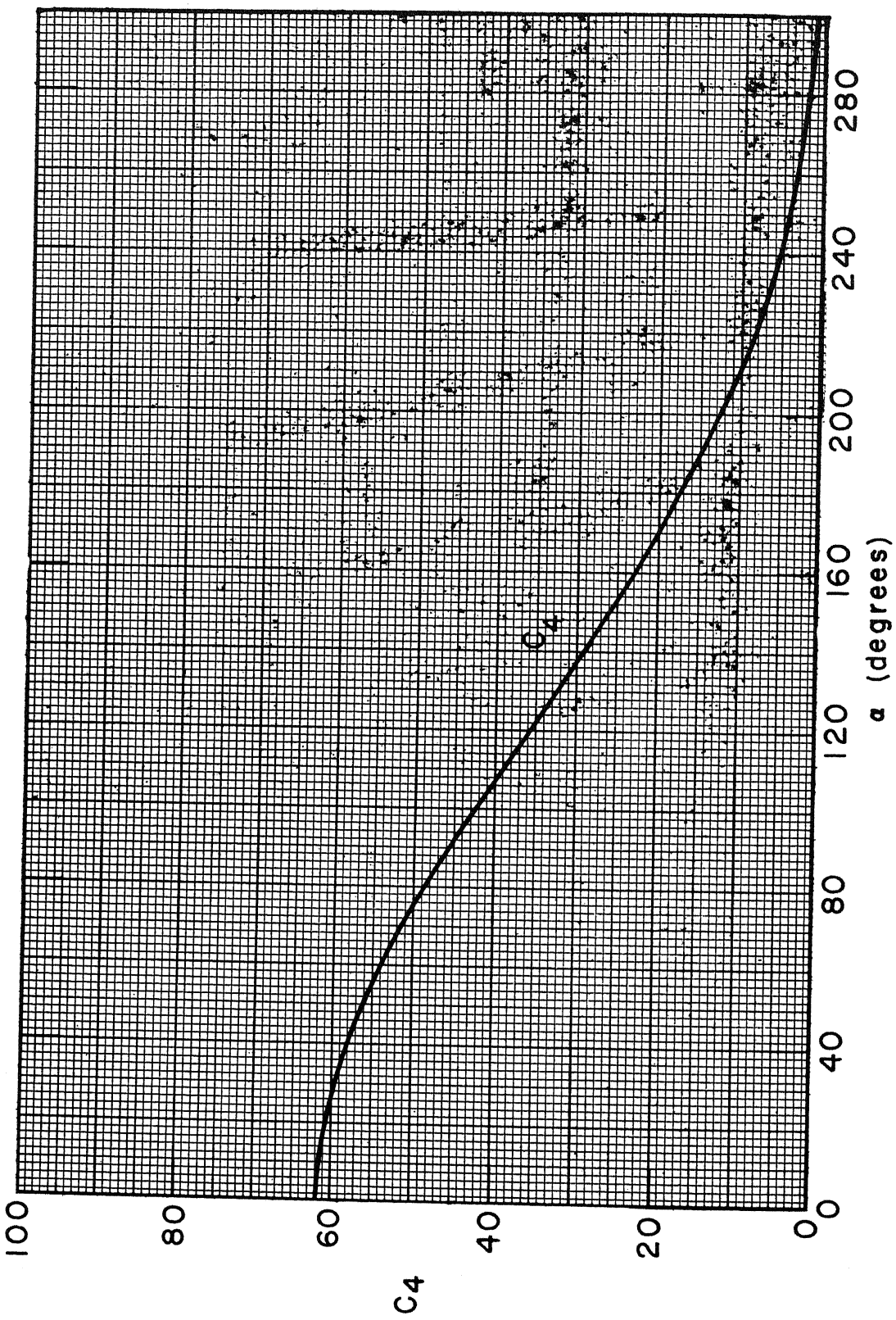

Figure 10.11. Vibration parameter C_4 as a function of the central angle α for a fixed-end arch in the deflection mode

rough approximation to the total impulse per unit area normal to the arch surface due to that modal loading is

$$H = (1.25 \text{ to } 1.50)\, P_{so} t_s \tag{10.13}$$

It is recommended that the larger coefficient be used in general for design purposes.

The effect of this impulse can be stated in terms of the period of the structure in the deflection mode T_{nd}, the yield resistance q, the deflection of the structure at yielding x_e, and the maximum deflection x_m. These deflections are illustrated in figure 10.12 and are measured normal to the arch axis, usually occurring at the quarter points of the arch where the deflection mode deflections are greatest.

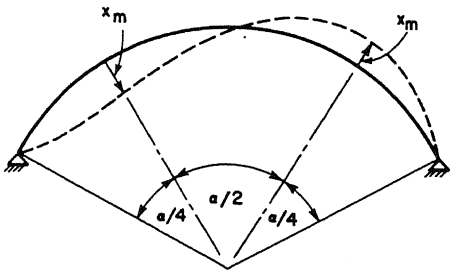

Figure 10.12. Location and direction of maximum deflections of an arch subjected to deflection mode loadings

In stating the relations that apply to the structure let the impulse be defined as follows:

$$H = p_i t_i \tag{10.14}$$

where t_i is arbitrarily chosen suitably small.

Using the energy approach method as outlined in paragraph 5-12 of EM 1110-345-415 the work done by the structure under the imposed loading is

$$W = E = \frac{(p_i t_i)^2}{2m_e} = qx_m - \frac{1}{2} qx_e \; R_m \left(x_m - \frac{1}{2} x_e\right)$$

assuming an idealized resistance diagram as shown in figure 10.13.

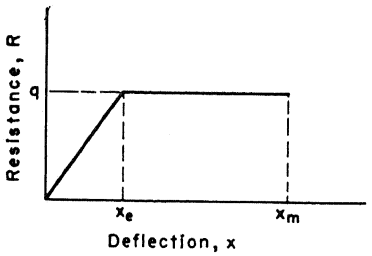

Figure 10.13. Idealized resistance function

Effective mass m_e can be related to the period of the structure by means of the relation

$$T_{nd} = 2\pi \sqrt{\frac{m_e x_e}{q}}$$

Combining the two preceding relations yields the equation

$$\frac{p_i}{q} (2\pi t_i / T_{nd}) = \sqrt{2 \frac{x_m}{x_e} - 1} \qquad (10.15)$$

This relation is strictly correct only if t_i approaches zero, but it is adequate for t_i as large as $0.2\ T_{nd}$. It is suggested that t_i be taken equal to $T_{nd}/2\pi$.

For allowable plastic deflections x_m exceeding the yield deflection x_e the equivalent static load at yielding, which is herein defined as the yield resistance, is given by:

$$q = \frac{2\pi}{T_{nd}} (1.5\ P_{so} t_s) \frac{1}{\sqrt{2 \frac{x_m}{x_e} - 1}} \qquad (10.16)$$

For allowable deflections not to exceed the yield deflection, that is $x_m \leq x_e$, the behavior will be entirely elastic and the equivalent static load $\bar{p}$ is given by the relation

$$\bar{p} = \frac{2\pi}{T_{nd}} (1.5\ P_{so} t_s) \qquad (10.17)$$

Equation (10.15) can be used to find either the desired resistance q , the impulse $H = p_i t_i$ that will just produce a certain deflection, or the ratio of the maximum to yield deflections x_m/x_e when the other quantities are given. Because of the freedom of choice of t_i , equation (10.15) is essentially only a relation between p_i/q and x_m/x_e , and the values are plotted in figure 10.14 for a value of $t_i = (1/2\pi)\ T_{nd}$

The time to reach the maximum deflection t_m can be approximated quite closely by the relation

$$t_m/T_{nd} = 0.091 + (p_i/q)\ (t_i/T_{nd}) \qquad (10.18)$$

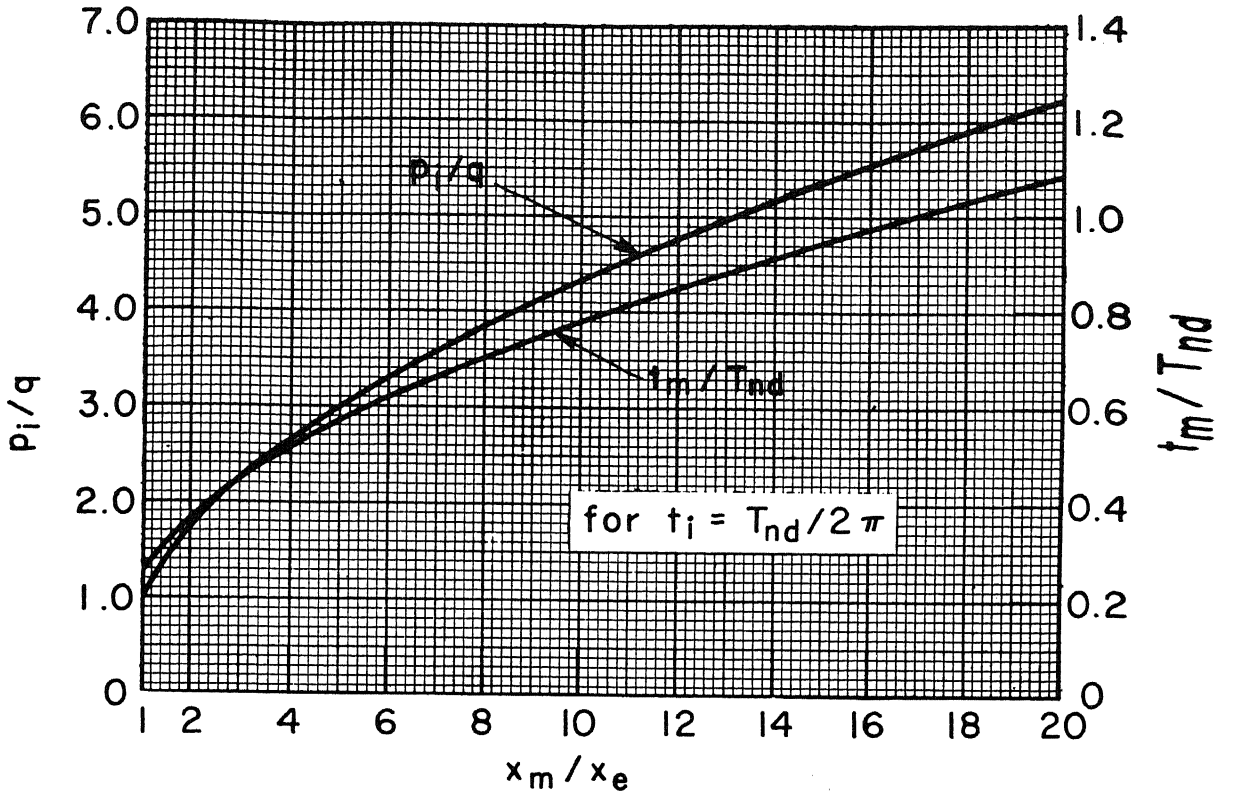

Figure 10.14. Relative values of parameters in the deflection mode

or for $t_i = (1/2\pi)\ T_{nd}$

$$t_m/T_{nd} = 0.091 + 0.159(p_i/q) \qquad (10.19)$$

Equation (10.19) is also plotted in figure 10.14.

c. Secondary Effects. There are related secondary effects which must be considered in the deflection and compression mode loadings and responses. In the compression mode there must be some flexure. However, if the arch section is designed so that yielding is nowhere present under compression mode loadings, the accompanying flexure in that mode will not cause collapse of the structure.

Another and more serious effect is the effect on the deflection under deflection mode loadings due to susceptibility of the arch to buckling under the compression mode loadings.

If a curved bar with hinged ends and with its center line in the form of an arc of a circle is submitted to the action of a uniform distributed

pressure P_{cr}, it will buckle as shown by the dotted line of figure 10.15. This tendency to buckle as shown will increase the deflections as computed under deflection mode loadings where buckling does not occur.

The uniform pressure that produces buckling is given by the relation [8]

$$P_{cr} = \frac{EI}{R^3}\left(\frac{4\pi^2}{\alpha^2} - 1\right) \tag{10.20}$$

If the ends of a uniformly compressed arch are built in, the shape of the buckling will be as shown by the dotted curve of figure 10.16. In this

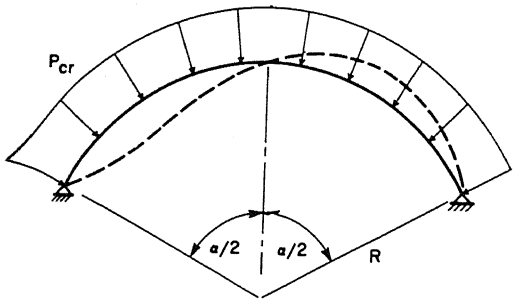

Figure 10.15. Buckled shape and distribution of critical pressure for a two-hinged arch

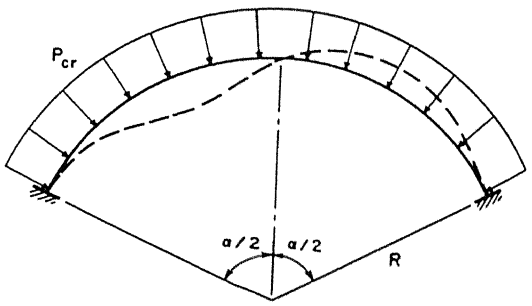

Figure 10.16. Buckled shape and distribution of critical pressure for a fixed-end arch

case also, the deflections of the deflection mode tend to increase due to the tendency of the arch to buckle under the uniform compressive loading of the compression mode.

The uniform pressure that produces buckling is given by the relation [8]

$$P_{cr} = \frac{EI}{R^3}(k^2 - 1) \tag{10.21}$$

where k is defined by the relation

$$k \tan \frac{\alpha}{2} \cot \frac{k\alpha}{2} = 1 \tag{10.22}$$

Figure 10.17 is a plot of k as a function of α.

If we designate by x_m the deflection in the deflection mode when

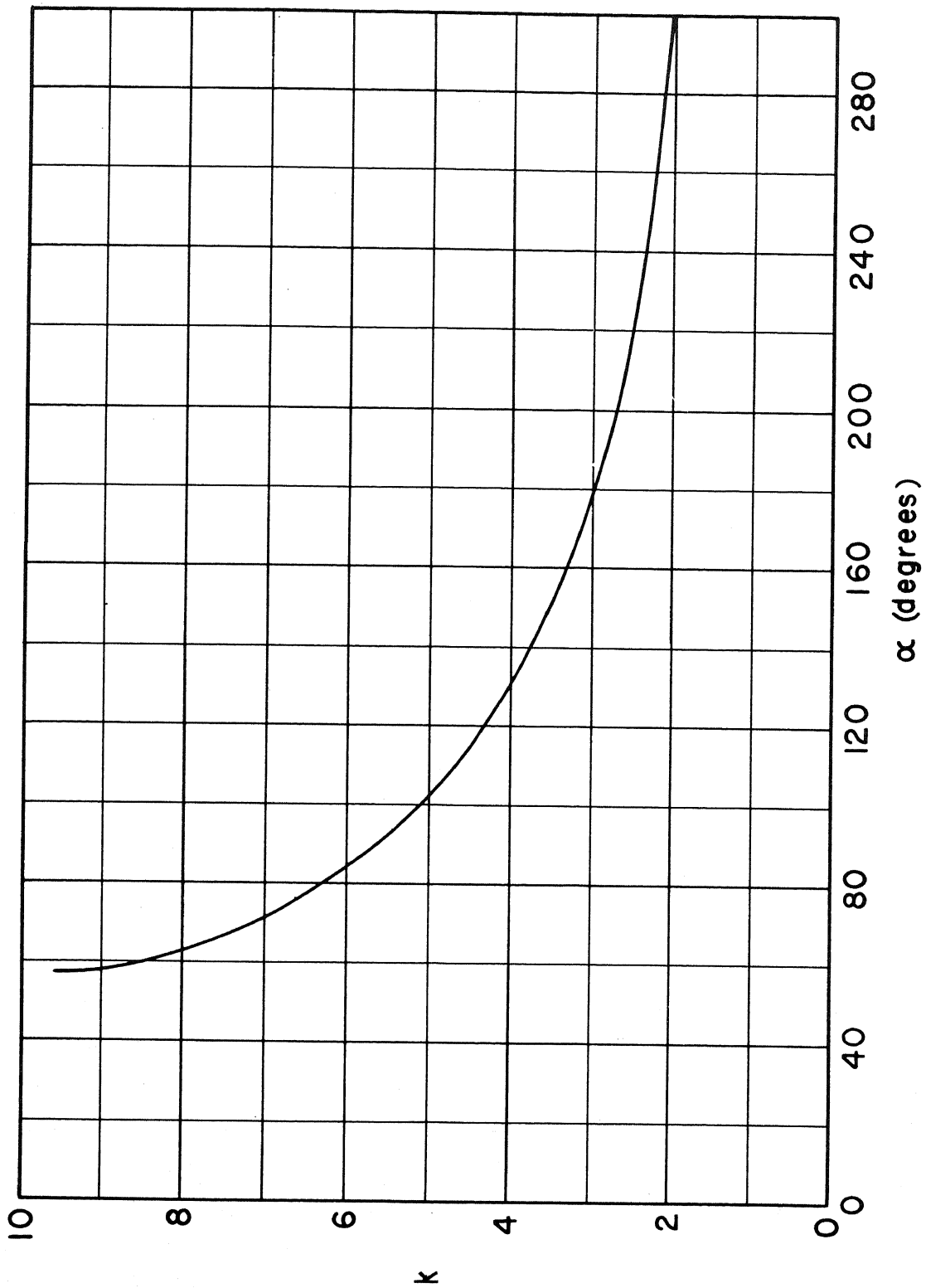

Figure 10.17. Buckling parameter k as a function of the central angle α for a fixed-end arch

there is no buckling load, and by $\bar{x}_m$ the deflection when there is a compressive force tending to produce buckling, the relation between these two deflections is given by

$$\frac{\bar{x}_m}{x_m} = \frac{\bar{x}_m/x_e}{x_m/x_e} = \frac{1}{1 - P_c/P_{cr}} \qquad (10.23)$$

where P_c is the compressive mode loading.

This relation is strictly applicable only for elastic behavior. Under dynamic conditions, the strength of the arch would be higher than under static conditions since it takes time for the arch to buckle. Equation (10.23) can be used as an approximation, with the average value of the compression mode loading over the time to reach maximum deflection in the deflection mode t_m used in the above equation for P_c

d. Response to Loading Produced by the Blast Wave Traveling Axially Along the Arch Axis. When a blast wave approaches normal to the end wall of the structure the loading on any ring is approximately instantaneous. Considering elastic behavior, since the duration of the load is long and the natural period of vibration of the structure is short, the dynamic load factor approaches two, that is, the stresses produced are twice those that would be produced by the same load applied statically. The resistance to this type of loading is primarily by means of direct stress in the arch. Since the axial stress produced by this loading is approximately constant over the length of the arch, yielding will not be confined to the development of plastic hinges at isolated points along the arch. Rather, plastic hinges of finite length, or better, plastic areas, will develop over those portions of the arch at which the stress is approximately equal to the dynamic yield strength of the material. This condition, if allowed to develop, will result in either large deflections of the arch or instability, neither of which can be tolerated. Both of these conditions may be considered as failure or collapse conditions. Thus, for an arch loaded by a blast wave traveling axially along the structure the response should be confined to elastic action only.

The period of the structure can be determined by those of equations (10.7) and (10.9) which are applicable. The relation between the natural

period and the duration of the dynamic loading allows the dynamic load factor to be determined from the charts presented in paragraph 5-10.

The adequacy of the structure against buckling should be checked by means of equation (10.20) or (10.21).

10-08 RELATIONS FOR ARCH ANALYSIS. a. General. To facilitate the design of arched elements, the following sections contain relations which will allow the analysis of arches without recourse to additional texts. References [4, 5, 6, and 9].

b. Two-Hinged Arch Relations, Deflection Mode Loading. Figure 10.18 illustrates the reactions developed by a two-hinged arch and the notation for the quantities involved in the deflection mode. From principles of symmetry and antisymmetry and applying the laws of statics

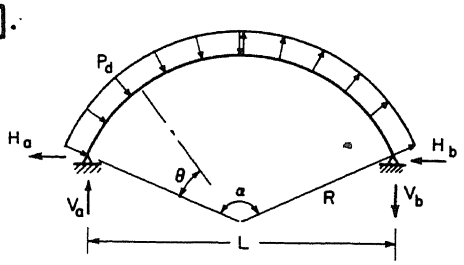

Figure 10.18. Deflection mode loading applied to a two-hinged arch

$$V_a = V_b = P_d \frac{R}{\sin \frac{\alpha}{2}} \left[\sin \frac{\alpha}{4} \sin \frac{3\alpha}{4} - \sin^2 \frac{\alpha}{4}\right] \qquad (10.24)$$

$$H_a = H_b = P_d R \left(1 - \cos \frac{\alpha}{2}\right) \qquad (10.25)$$

At any point on the arch defined by the angle θ, the bending moment M_θ is given by, for $\theta < \frac{\alpha}{2}$,

$$M_\theta = V_a \left[R \left(\sin \frac{\alpha}{2} - \left[\sin \frac{\alpha}{2} - \theta\right]\right)\right] + H_a \left[R \left(\cos \left[\frac{\alpha}{2} - \theta\right] - \cos \frac{\alpha}{2}\right)\right] - P_d (2R^2) \sin^2 \frac{\theta}{2} \qquad (10.26)$$

Since shear = $dM/ds = dM_\theta/Rd_\theta = V_\theta$

$$V_\theta = V_a \cos \left(\frac{\alpha}{2} - \theta\right) + H_a \sin \left(\frac{\alpha}{2} - \theta\right) - P_d (2R) \sin \frac{\theta}{2} \cos \frac{\theta}{2} \qquad (10.27)$$

c. Two-Hinged Arch Relations, Compression Mode Loading. Figure 10.19 illustrates the reactions developed by a two-hinged arch and the notation for quantities involved in the compression mode.

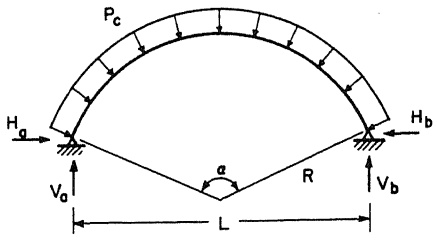

Figure 10.19. Compression mode loading applied to a two-hinged arch

From principles of symmetry and the laws of statics

$$V_a = V_b = P_c R \sin \frac{\alpha}{2} \qquad (10.28)$$

This structure is statically indeterminate to the first degree and principles of statically indeterminate structural analysis must be resorted to. In some cases, the effect of axial distortion will appreciably affect the values of the quantities to be determined. For arches loaded radially this effect is small and hence is neglected. Therefore, the applied load is carried by axial thrust only, and

$$H_a = H_b = P_c R \cos \frac{\alpha}{2} \qquad (10.29)$$

and the axial thrust is given by the relation

$$T = P_c R \qquad (10.30)$$

d. Fixed-End Arch Relations, Deflection Mode Loading. Figure 10.20 illustrates the reactions developed by a fixed-end arch and the notation for quantities in the deflection mode. From considerations of antisymmetry and the laws of statics

$$H_a = H_b = P_d (2R) \sin^2 \frac{\alpha}{4} \qquad (10.31)$$

and also

$$M_a = M_b \; ; \quad V_a = V_b$$

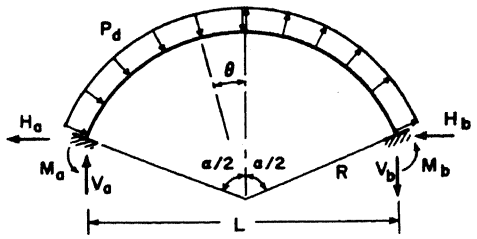

Figure 10.20. Deflection mode loading applied to a fixed-end arch

This structure is indeterminate to the first degree. Assuming that the flexural distortion is large compared with the axial distortion simplifies the analysis of this structure without introducing appreciable error. If the shear existing at the center of the arch is known, all other

quantities are easily found. This shear is denoted by V_c and is considered to be positive when acting upward on the left-hand portion of the arch. Then

$$V_c = RP_d \frac{\left[\cos\alpha - 4\left(\cos\frac{\alpha}{2}\right) + 3\right]}{\alpha - \sin\alpha} \qquad (10.32)$$

and

$$V_a = V_b = 2P_d R \sin\frac{\alpha}{4}\cos\frac{\alpha}{4} - V_c \qquad (10.33)$$

and

$$M_a = M_b = 2P_d R^2 \sin^3\frac{\alpha}{4} - V_c R \sin\frac{\alpha}{2} \qquad (10.34)$$

The moment at any point in the arch, defined by the angle θ, is

$$M_\theta = RV_c \sin\theta - 2P_d R^2 \sin^2\frac{\theta}{2} \qquad (10.35)$$

Since shear $= V_\theta = dM_\theta/Rd_\theta$

$$V_\theta = V_c \cos\theta - 2P_d R \sin\frac{\theta}{2}\cos\frac{\theta}{2} \qquad (10.36)$$

e. Fixed-End Arch Relations, Compression Mode Loading. Figure 10.21 illustrates the reactions developed by a fixed-end arch and the notation for quantities involved in the compression mode. This structure is indeterminate to the second degree, but assuming here, as in paragraph 10-08c, that the effect of axial distortion on the reactions can be neglected greatly simplifies the expressions obtained without introducing any appreciable error. Making this assumption yields, for the vertical reactions

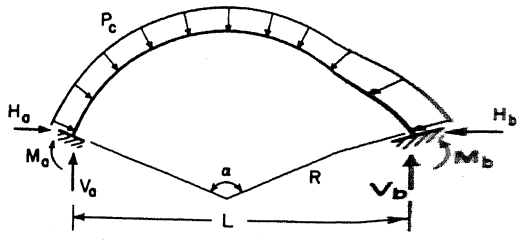

Figure 10.21. Compression mode loading applied to a fixed-end arch

$$V_a = V_b = P_c R \sin\frac{\alpha}{2} \qquad (10.37)$$

for the horizontal reactions

$$H_a = H_b = P_c R \cos \frac{\alpha}{2} \qquad (10.38$$

for the thrust

$$T = P_c R \qquad (10.39$$

The moment reactions M_a and M_b are equal to zero.

10-09 DESIGN PROCEDURE. a. General. The design procedure is outlined below. If the direction of the approaching blast wave with respect to the structure is known, only the applicable procedure outlined below need be applied. If the blast wave may approach from any direction, the two critical orientations, the blast wave normal to the arch axis and the blast wave parallel to the arch axis, must both be considered, as either may determine the arch dimensions. For this situation it is recommended that the arch be designed for load in one direction and then this section be analyzed for the load in the other direction.

b. Design Procedure for the Blast Wave Normal to the Arch Axis.

Step 1. Determine the size and shape of the arch and the value of the incident overpressure P_{so}. The ratio of the maximum deflection to the elastic deflection is selected by considering the degree of damage to be permitted. Recommendations as to the values of these ratios for various degrees of damage are given in paragraph 6-26.

Step 2. The pressure vs time relations for several points on the arch are determined by the methods given in paragraph 3-17. From these pressure vs time relations the values of the compression P_c and deflection P_d modal loadings may be determined. If it has been decided that the use of these more exact methods of load determination are unwarranted, the approximate values for these quantities as given in figure 10.4 may be used.

Step 3. Determine the total impulse in the deflection mode by taking the area under the P_d vs time curve. In using the actual P_d vs time curve, the value of P_d becomes very small for times in excess of $2.5\ t_s$, hence the impulse beyond this time can be neglected. If the

approximate modal loadings of figure 10.4 are used, the impulse can be determined by applying equation (10.13).

Step 4. Assume a depth of the arch and a reinforcement pattern (a value of $p = 0.015$ is recommended as an initial trial) and compute the average moment of inertia (defined as one-half the sum of the transformed and gross moments of inertia).

Step 5. Determine the maximum moment in terms of the unit resistance q using the arch relations of paragraph 10-08.

Step 6. Determine the resisting moment of the arch section by the methods of paragraph 4-11 taking into account the axial load on the arch cross section. By deducting the dead load moment from this resisting moment determine the resisting moment available for blast loading.

Step 7. Determine the value of the unit resistance q in the deflection mode by equating the maximum moment in terms of q to the resisting moment available for blast loading.

Step 8. Compute the natural period of the arch in the deflection mode using equation (10.11) or (10.12).

Step 9. Compute the values of t_i and p_i by the methods of paragraph 10-07b. From figure 10.14 determine values of x_m/x_e and t_m/T_{nd}. The value of the time to reach maximum deflection t_m can be found and compared with $t = 2.5\ t_s$ (see step 3 above). If t_m is greater than $2.5\ t_s$, the procedure in step 3 is satisfactory. If t_m is less than $2.5\ t_s$, then only the impulse up to time t_m should be used in computing p_i. It is not likely that t_m will be less than $2.5\ t_s$ for arch structures.

Step 10. Determine the values of $\bar{x}_m/x_e$ from equation (10.23). Compare this with the value selected in step 1, and if necessary, adjust the design to make the actual value of $\bar{x}_m/x_e$ compare more closely with the design value.

c. Design Procedure for Blast Wave Along the Arch Axis - ELASTIC ACTION ONLY. Step 1. Determine the size and shape of the arch and the value of the incident peak overpressure P_{so}

Step 2. Determine the pressure vs time relations for a ring of the arch normal to the arch axis by the procedures given in paragraph 10-06b.

Step 3. Assume a depth of the arch and reinforcement pattern (a value of $p = 0.015$ is recommended as an initial trial) and compute the average moment of inertia (defined as one-half the sum of the transformed and gross moments of inertia).

Step 4. Compute the natural period of vibration for the arch using equations (10.7) to (10.10).

Step 5. Idealize the loading curve obtained in step 2 by the methods presented in paragraph 5-13.

Step 6. Determine the dynamic load factor for the arch from the curves of paragraph 5-12.

Step 7. Since the duration of the idealized load is large compared to the natural period of vibration, the arch responds rapidly to the applied dynamic loads. Therefore, the arch should be analyzed for the dead load plus the dynamic load factor times the peak value of the dynamic load acting as a static load. The maximum stress in the arch should not be allowed to exceed the dynamic yield strength of the material of which the arch is composed. If the stresses are greater or much less than these allowable values the trial section of step 3 must be revised assuming this to be the factor that controls the design.

Step 8. Check this section to see that there is no danger of buckling under the imposed dynamic loading by means of equation (10.20) or (10.21).

10-10 DESIGN OF REINFORCED-CONCRETE BARREL ARCH. a. General. To illustrate the design procedures set forth in this manual, the methods presented will be applied to the design of a two-hinged semicircular barrel arch of reinforced concrete. Two structures will be designed: one for the blast load approaching normal to the axis of the structure and the other for the blast load approaching along the axis of the structure. This approach is followed since it is possible for the orientation of the structure to be such that the blast can approach from only one of these directions. With this approach the design procedures associated with each orientation are more completely illustrated. If the structure is to be designed so that it must be resistant to blast loads approaching in any direction, then the structure should be designed for one orientation and analyzed for the

other. Usually, deflection criteria determine the design of the structure for the blast wave normal to the axis and stress criteria determine the design when the blast wave approaches parallel to the axis. Only the design of the arched elements is illustrated here. The design in each case is carried out for a typical ring 12 in. in width. The length of the structure is taken to be 60 ft and no intermediate diaphragms are present, or if present, they are not spaced so closely as to influence the response of the arch.

b. Design of a Two-Hinged Arch, Blast Wave Normal to the Arch Axis.

Step 1. The size and shape of the arch and the support conditions are illustrated in the accompanying sketch. The arch is to resist a maximum incident overpressure P_{so} equal to 10 psi with a duration of positive phase t_o equal to 0.685 sec. The ratio of maximum deflection to elastic deflection under these loads $\bar{x}_m/x_e$ is not to exceed 10.

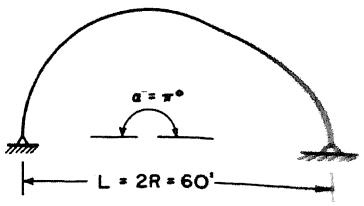

Step 2. The deflection and compression mode loadings are determined from the approximate curves illustrated in figure 10.4 and are shown in figure 10.22. The transit time of the shock wave is found to be

$$t_s = R/U_o = 60/1400 = 0.043 \text{ sec}$$

where U_o, the velocity of the shock front, is found to be 1400 fps from figure 3.9.

Step 3. The total impulse in the deflection mode is given by equation (10.13)

$$H = 1.5\, P_{so} t_s = 1.5(10)0.043 = 0.646 \text{ lb-sec/in.}^2$$

Step 4. Assume a total arch thickness of 10 in. with a percentage of reinforcement equal to 1.5 percent in each face.

$$A_s = A'_s = 10(12)0.015 = 1.8 \text{ in.}^2$$

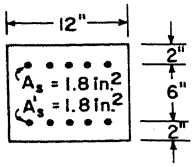

Intermediate grade steel, $f_{dy} = 52{,}000$ psi

3000-psi concrete, $f'_{dc} = 3900$ psi

Gross $I = 1000 \text{ in.}^4$

Transformed $I = 572 \text{ in.}^4$

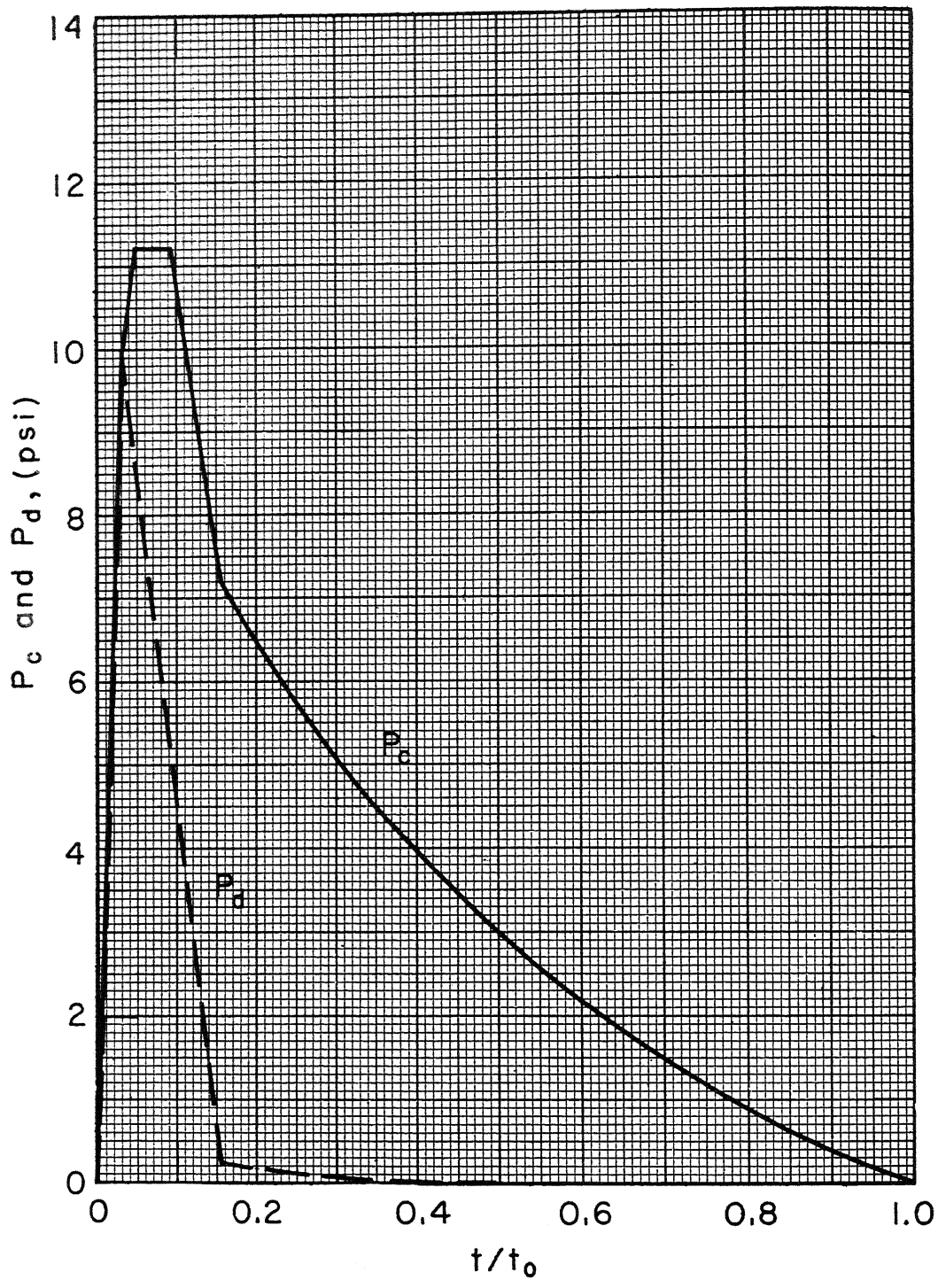

Figure 10.22. Compression and deflection mode loadings

Average $I = 786$ in.^{4}

Dead weight of 1-ft-wide strip $= 10(12)150/144$

$= 125$ lb/ft

Mass per in. of circumferential length $= 125/(32.2)144$

$= 0.0269$ lb-sec^2/in.^{2}

Step 5. The moment in terms of the yield resistance q due to deflection mode loadings can be found from the relations of paragraph 10-08b.

$$V_a = V_b = q\,R \csc\frac{\alpha}{2}\left(\sin\frac{\alpha}{4}\sin\frac{3\alpha}{4} - \sin^2\frac{\alpha}{4}\right)$$

$$V_a = V_b = 0 \qquad \text{(eq 10.24)}$$

$$H_a = H_b = q\,R\left(1 - \cos\frac{\alpha}{2}\right) = q\,R \qquad \text{(eq 10.25)}$$

The maximum moment occurs at the point of zero shear. Equating equation (10.27) to zero yields

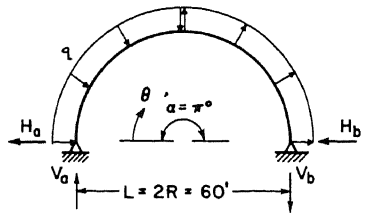

$$0 = R\,q\sin(\pi/2 - \theta) - q\,2R\sin\frac{\theta}{2}\cos\frac{\theta}{2}$$

$0 = \cos\theta - \sin\theta$ and $\theta = 45^\circ$

At the point defined by $\theta = 45^\circ$ the moment is given by equation (10.26)

$$M_\theta = q\,R^2\cos 45^\circ - q\,2R^2\sin^2 45^\circ/2 = 0.414\,q\,R^2$$

Step 6. In order to evaluate the resisting moment of the section it is necessary to know the axial thrust which is present in the arch. This thrust is dependent upon the average value of the compression mode loading existing on the structure over the time required to reach maximum deflection. Assume initially that this average value of P_c existing over time t_m is 6.0 psi. The analysis of the arch under the compression mode loading can be obtained by application of the relations of paragraph 10-08c.

From equation (10.30)

T = thrust $= P_c R = 6(144)30 = 25{,}900$ lb

Dead load horizontal thrust $= (1/2)wR = (1/2)(125)30$

$= 1875$ lb [4, 5]

Dead load vertical shear at $\theta = 45^\circ = (1/4)\pi\,Rw$

$= 0.785(30)125 = 2940$ lb

Dead load axial thrust $= \cos 45^\circ(1875 + 2940) = 3410$ lb

Total axial thrust P_D at $\theta = 45^\circ = 25.9 + 3.4 = 29.3$ kips

From equation (4.32) the resisting moment of the arch at the quarter point of the arch is

$$M_D = A_s d' f_{dy} + P_D \left(\frac{t}{2} - \frac{P_D}{1.7\, b f'_{dc}} \right)$$

$$= 1.62(6)52 + 29.3 \left[(10/2) - \frac{29.3}{1.7(12)3.9} \right]$$

$$= 562 + 136 = 698 \text{ in.-kips}$$

Dead load moment at the quarter point [6]

$$= 1/2\, \pi\, wR\, (1 - 0.707)\, R - 1/2\, wR\, (0.707)\, R - w \int_0^{\pi/4} R\, (\cos\theta - 0.707)\, R\, d\theta$$

$$= -0.045\, wR^2 = -0.045(125)30^2(12) = -61 \text{ in.-kips}$$

Resisting moment available for blast load M_a

$$M_a = 698 - (-61) = 759 \text{ in.-kips}$$

Step 7. The unit resistance in the deflection mode is obtained by equating the maximum moment of step 5 to the available resisting moment of step 6.

$$0.414\, qR^2 = M_a$$

$$q = \frac{759{,}000}{0.414(30^2)1728} = 1.18 \text{ psi}$$

Step 8. The natural period of the structure is given by equation (10.11)

$$T_{nd} = \frac{2\pi L^2}{C_3} \sqrt{\frac{m}{EI}}$$

where, from figure 10.9, $C_3 = 8.9$

$$T_{nd} = \frac{2\pi(720^2)}{8.9} \sqrt{\frac{0.0269}{3(10^6)786}}$$

$$= 1.24 \text{ sec}$$

Step 9. From paragraph 10-07b

$$t_i = T_{nd}/2\pi = 1.24/6.28 = 0.197 \text{ sec}$$

$$p_i = H/t_i = 0.646/0.197 = 3.28 \text{ psi}$$

$$p_i/q = 3.28/1.18 = 2.78$$

From figure 10.14 $x_m/x_e = 4.4$

$t_m/T_{nd} = 0.56$, $t_m = 0.56(1.24)$

$= 0.69$ sec

From figure 10.22, the average value of P_c over time t_m is found to be approximately 5 psi. The assumed value in step 6 was 6.0 psi. This means that the resisting moment available for blast loading is less than the value obtained in step 6. The change in this resisting moment is not too great, so in this instance the design from step 6 on will not be revised. If the error in the assumed average value of P_c produces large changes in M_a it should be accounted for.

Step 10. The buckling load is given by equation (10.20)

$$P_{cr} = \frac{EI}{R^3}\left(\frac{4\pi^2}{\alpha^2} - 1\right) = \frac{3(10^6)786}{360^3}(3) = 15.2 \text{ psi}$$

From equation (10.23) the maximum deflection is found to be

$$\bar{x}_m/x_e = (x_m/x_e)\frac{1}{(1 - P_c/P_{cr})} = 4.4\frac{1}{(1 - 5/15.2)} = 6.6$$

Since the computed value of $\bar{x}_m/x_e = 6.6$ is less than the maximum specified value in step 1 the design is satisfactory.

c. Blast Wave Approaching Along the Arch Axis. Step 1. The size and shape of the arch is that given in the preceding section. The radius is 30 ft with an interior angle of 180^o. The maximum incident overpressure P_{so} is 10 psi, and the duration of the positive phase is 0.685 sec.

Step 2. The pressure vs time relation is that given in paragraph 10-06b. Considering a strip 1 ft wide the rise time is given by

$$t_r = 1/U_o = 1/1400 = 1 \text{ msec}$$

where U_o is the velocity of the shock front obtained from the curves of figure 3.9. Since the rise time is very small it may be neglected. The loading is then given by the relation

$$P(t) = P_{so}(1 - t/t_o)\, e^{-t/t_o} = 10(1 - t/0.685)\, e^{-t/0.685}$$

This relation is tabulated in table 3.1 and the overpressure curve so obtained is plotted in figure 10.23.

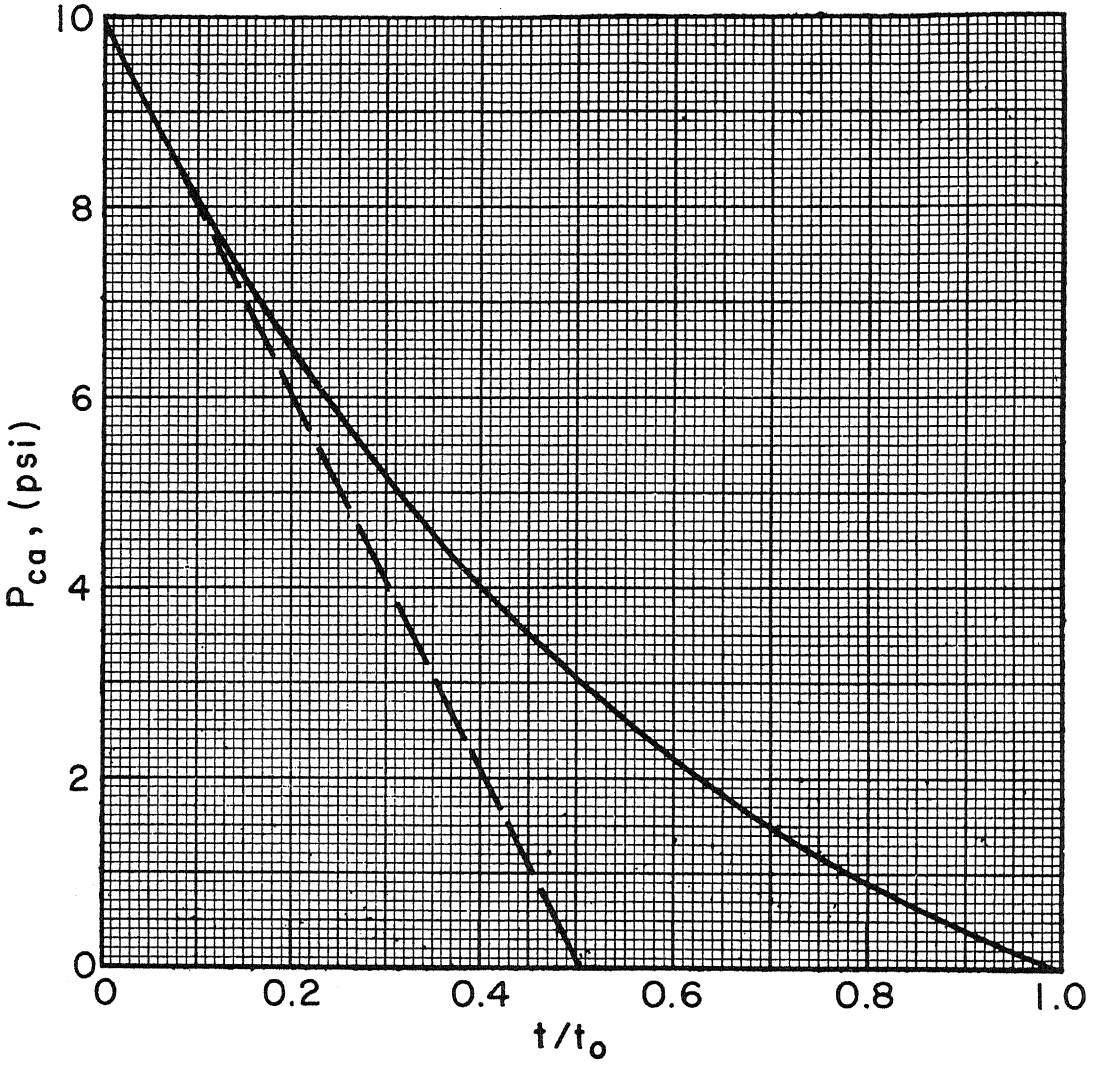

Figure 10.23. Radial compressive load

Step 3. The depth of the arch is assumed to be 10 in. with $A_s = A'_s = 1.80$ in.^{2} This is the same cross section assumed in paragraph 10-10b and the structural properties may be obtained from that section.

Step 4. The natural period of vibration in the compression mode is given by equation (10.7)

$$T_n = \frac{2\pi L^2}{C_1}\sqrt{\frac{m}{EI}}$$

where

$$C_1 = 4\sin^2\frac{\alpha}{2}\sqrt{0.820(R/k)^2 + \left(\frac{\pi^2}{\alpha^2} - 1\right)^2}$$

$L = 720$ in.

$R = 360$ in.

$m = 0.027$ lb-sec^2/in.^{2}

$I_a = 786$ in.^{4}

$E = 3 \times 10^6$ psi

$A_g = 120$ in.^{2}

$A_t = 90$ in.^{2}

$A_a = 105$ in.^{2}

$k = \sqrt{I_a/A_t} = 2.96$ in.

$$C_1 = 4\sqrt{0.820(360^2)/(2.96^2)} = 442$$

$$T_n = \frac{2\pi 720^2}{442}\sqrt{\frac{0.027}{3(10^6)786}} = 0.027 \text{ sec}$$

Step 5. The load vs time curve of figure 10.23 is idealized by a triangular pulse shown by the dashed line. The duration of this pulse T is 0.5 t_o equal to 0.343 sec.

Step 6. From steps 4 and 5, $T/T_n = 12.71$. From figure 5.20 the dynamic factor is found to be 2.0.

Step 7. From figure 5.20 it is seen that the response of the structure is so rapid for this large value of T/T_n that the dynamic load factor is independent of the shape of the idealized load curve. Hence the average load applied over time t_m is the peak load $P_{so} = 10$ psi. Therefore, the structure is analyzed for a static load equal to the dynamic load factor times P_{so} equal to 20 psi plus the dead load.

Due to the dynamic radial compressive load of 20 psi, a uniform axial thrust is produced in the arch. From equation (10.30) this thrust is found to be

$$T = D.L.F.(P_c R) = 2(10)144(30) = 86.4 \text{ kips}$$

From paragraph 10-10b the axial thrust due to the dead load of the arch is 3.41 kips and the bending moment is 61.0 in.-kips, these being the maximum values of these quantities which occur at the quarter point of the arch. Therefore, the total axial thrust P_D is

$$P_D = 86.4 + 3.4 = 89.8 \text{ kips}$$

and the total bending moment is

$$M = 61.0 \text{ in.-kips}$$

The maximum concrete stress produced by these loads is

$$f_c = (P/A) + (Mc/I) = (89.8/120) + [61(5)/786]$$
$$= 0.75 + 0.39 = 1.24 \text{ kips/in.}^2$$

Step 8. The buckling load is the same as that computed in paragraph 10-10b and is

$$P_{cr} = 15.2 \text{ psi}$$

This value is less than the applied dynamic load times the dynamic load factor. Since it takes time for the arch to buckle and since the dynamic load attenuates rapidly, this design might be considered as satisfactory. To be on the safe side the arch should be increased in depth to 11 in. thus raising the buckling to slightly more than 20 psi.

DOMES

10-11 TYPES OF STRUCTURES CONSIDERED. The domes considered in this manual are surfaces of revolution formed by revolving an arc of a circle whose center is on the axis of rotation. These structures are circular in plan view. This type of structure is generally reinforced along its support by a ring beam which resists the thrust of the dome by tension in the ring.

In all the domes considered in this manual the surface is monolithic, no ribs or other supporting elements are considered as being effective in resisting the external loads. The structures are also assumed to be closed, thus preventing the development of any internal pressures.

The method presented requires that the dome resist the applied blast loads by ELASTIC ACTION only.

10-12 TYPES OF LOADING. The loading of domes is divided into two

components: (1) symmetrical or "compression mode" loading, and (2) anti-symmetrical or "deflection mode" loading. Only one modal response of each type is considered.

The modal loadings are determined by using the average intensities of blast pressure over the windward and leeward halves of the dome. The curve of blast loading vs time for any point on the dome is obtained by the methods of paragraph 3-19. The average intensity over each half of the dome is obtained from these individual load vs time curves for several points on the surface of the dome. Consider the dome shown in figure 10.24. The average overpressures on the windward and leeward sides of the dome can be determined by averaging the overpressures existing on meridional strips for different β angles. The work involved in determining these average pressures can be reduced if advantage is taken of the rotational symmetry of the dome, that is, choosing β and α values which are symmetrical about axes x-x and y-y, respectively. It is suggested that load vs time curves be determined for α values of 15°, 45°, 75°, 105°, 135°, and 165°, in the case of a hemispherical dome, on meridional strips having β values of 22.5°, 67.5°, 112.5°, and 157.5°. Due to rotational symmetry, the load vs time curves for points having β values of 22.5° and 67.5° will be the same as those for corresponding points having β values of 157.5° and 112.5°, respectively. The average pressure vs time curve over the windward side of the dome can be obtained by applying the trapezoidal integration formula to these load vs time curves, which results in a normal arithmetical averaging of intensities on the windward side due to the given selection of β and α values. The average pressure curve for the leeward side is similarly obtained.

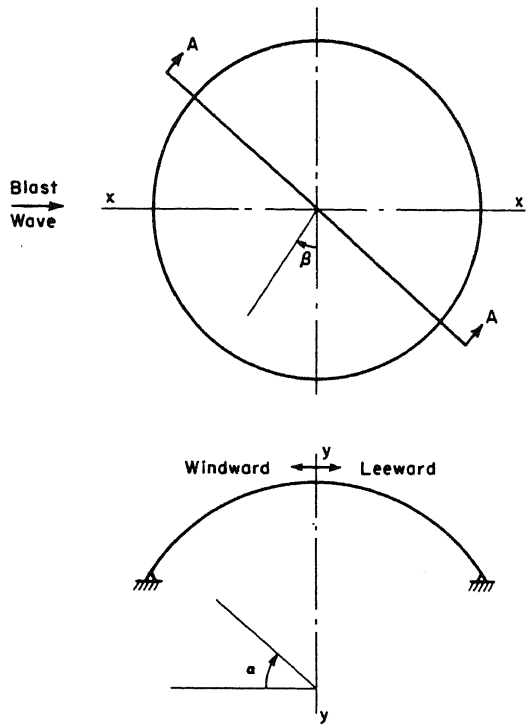

Figure 10.24. Plan and sectional views of a typical dome

The compression and deflection mode loadings are obtained by the same method as outlined in paragraph 10-06d. Denoting the average pressure on the windward side of the dome by P_n and that on the leeward side by P_f, the compression and deflection mode loadings are given by the relations:

$$\left.\begin{aligned} P_c &= 0.5\,(P_n + P_f) \\ P_d &= 0.5\,(P_n - P_f) \end{aligned}\right\} \qquad (10.40)$$

As is stated later in paragraph 10-13, the maximum values of P_c and P_d are of primary interest; therefore, the curves of load vs time for various points on the dome need only be computed for a duration of time equal to about twice the transit time of the shock wave over the dome.

10-13 STRUCTURAL RESISTANCE. a. Response to Compression Mode Loading. In the compression mode, the dome is very stiff and the period of vibration is consequently very short. For a complete spherical shell of constant thickness, the period T_c in seconds, is found to be [10]:

$$T_c = 2\pi \sqrt{\frac{mR^2\,(1 - \nu)}{2\,Eh}} \qquad (10.41)$$

where

m = the mass per unit surface area of the dome in lb-sec^2/in.^{3}

R = the radius of the dome in in.

ν = Poisson's ratio

E = the modulus of elasticity in lb/in.^{2}

h = the dome thickness in in.

The period for a structural dome is different from that given by equation (10.41) due to the fact that the shells considered herein are not completely spherical and are also influenced by the support conditions. The exact relation for the period of a dome which is not completely spherical has not been determined. The exact value is not important, since it is seen from equation (10.41) that the period is very short. The modal loadings to which a dome is subjected have rise times of the same order of

magnitude as the transit time of the shock wave over the structure. The ratio of the rise time to the period is large, and as can be seen from figure 5.21 the stresses that are produced by this dynamic loading are the same as those that would be produced by the peak value of the compression mode loading applied statically.

b. Response to Deflection Mode Loading. No solution has as yet been obtained for the period of a dome subjected to deflection mode loadings. The dome resists deflection mode loadings by developing internal forces in the plane of the surface. Thus resistance to this antisymmetrical loading is accomplished primarily by axial deformation rather than by bending of the dome. The period under this type of loading is therefore likely to be of the same order of magnitude as that under the compression mode loadings. Recognizing that the period is short, the exact value is not important.

The rise time of the deflection mode loading is of the same order of magnitude as the transit time of the shock wave. Therefore, the stresses produced by the dynamic loading are the same as those obtained by the peak deflection mode loading applied statically.

c. Combined Response to Modal Loadings. The relations for the analysis of a dome as presented in paragraph 10-15 are somewhat approximate in nature since a rigorous analysis involving compatibility of strains and the development of bending stresses in the vicinity of the supports is not in keeping with the approximations involved in the determination of the applied dynamic loads. Due to this fact, it is recommended that the sum of the maximum intensities of stress due to dead weight loading and compression and deflection mode loadings not exceed 0.8 of the dynamic yield strength of the steel or 0.8 of the dynamic cylinder strength of the concrete. It is further suggested that in the case of reinforced-concrete domes, that reinforcement be provided in both the meridional and latitudinal planes.

d. Secondary Effects. There may be a tendency for the dome to buckle under the uniform compression mode loadings. The critical uniform radial pressure causing buckling of a complete sphere is given by the relation [8]

$$P_{cr} = \frac{2\,Eh^2}{R^2\sqrt{3(1-\nu^2)}} \qquad (10.42)$$

where the quantities are as defined in equation (10.41).

Experimental verification of the above relation has not been achieved, the domes usually buckling under loads approximately 1/3 to 1/4 that given by equation (10.42). Research carried out by Von Karman and Tsien on spherical segments indicates a critical radial pressure [13]

$$P_{cr} = 0.4\,\frac{Eh^2}{R^2} \qquad (10.43)$$

assuming Poisson's ratio equal to zero. Equation (10.43) also assumes that the solid angle of the segment is not large.

For a spherical segment with R = 100 ft, h = 5 in., and $E = 3 \times 10^6$ psi, the critical pressure given by equation (10.43) is approximately 21 psi. Thus it appears that buckling under compression mode loadings is not likely to become a problem. Since the dome will require time to buckle under dynamic loads the compression mode loadings may approach the critical buckling pressure much more closely than would be the case if the same load were applied statically. It is recommended that the peak value of the compression mode loading not exceed the critical overpressure as given by equation (10.43).

10-14 RELATIONS FOR DOME ANALYSIS. a. General. The expressions presented here are for domes which are surfaces of revolution. The surface of the dome is described by revolving an arc of a circle whose center is on the axis of rotation.

b. Gravity Loads. The gravity loads considered on these domes are (1) uniform load per square foot of dome surface, and (2) variable load equal to zero at the top and increasing at a uniform rate toward the base. In either case, the load is constant along any circle of latitude or "hoop."

Normal design of domes is based on the assumption that they are so thin that they cannot develop bending moment, yet they are assumed to be so thick that there is no danger of buckling. Only shapes and loads which are symmetrical about the axis of rotation are taken into account, and stresses

due to wind pressure, volume change, and support displacement are ignored. No theory is now available that permits simple treatment of concentrated or unsymmetrical loadings; consequently, shells are not designed to carry loads of either of these two types.

The formulas in this paragraph apply only at points of domes which are removed some distance from the discontinuous edges. At the edges, the results from the formulas are indicative, but they do not accurately represent the stresses developed at those points. The edge member and the adjacent hoop of the shell must have very nearly the same strain when they are cast integrally. The significance of this fact is ignored in the relations and the forces are subject to certain modifications, not here discussed.

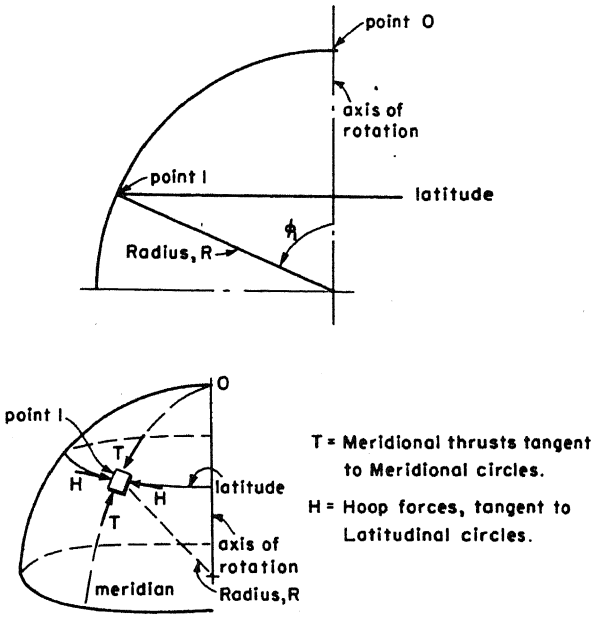

Figure 10.25. Definitive sketch for dome analysis under gravity loads

Consider part of the dome between planes of latitude through points 0 and 1 in figure 10.25.

$$\text{Surface area:} \quad A = 2\pi R^2 (1 - \cos \phi_1)^* \tag{10.44}$$

If the load per square foot of dome is uniform, w psf ,

$$\text{Total load:} \quad W_u = 2\pi R^2 w (1 - \cos \phi_1) \tag{10.45}$$

If the load increases from zero at point 0 at a rate of w' lb per radian

$$\text{Total load:} \quad W_v = 2\pi R^2 w' (\sin \phi_1 - \phi_1 \cos \phi_1) \tag{10.46}$$

---

* For derivation of these relations see reference [12].

Investigating the forces at the plane of latitude through point 1, W being the total load above that circle:

$$\text{Meridional thrust:} \quad T = \frac{W}{2\pi R \sin^2 \phi_1} \tag{10.47}$$

$$\text{Hoop force:} \quad H = -T + (w + w' \phi_1) R \cos \phi_1 \tag{10.48}$$

In these expressions a minus sign indicates tension. If the dome is discontinued along the circle of latitude through point 1, an edge member must be provided along that circle, and that member is subject to,

$$\text{Ring tension:} \quad S = - \frac{W \cos \phi_1}{2\pi \sin \phi_1} \tag{10.49}$$

The shell itself may be able to take this ring tension; but if an edge member is provided and cast integrally with the shell, it is customary to design it for the full amount of the force S

At the top of the solid dome:

$$T = H = 1/2 \; wR \tag{10.50}$$

In the design of a dome, a question arises concerning allowable stress in compression. Present practice is to permit a stress in concrete of about 200 psi. It appears that there is no theoretical reasoning behind these limiting figures, and codes do not usually state anything about stresses in domes; they are based merely on trends in past and present practice.

The relations in this section are included to allow an easy selection of an initial trial size for the dynamic design as well as to allow the determination of the stresses due to dead loads. It should be remembered in connection with this trial size that the shell must be thick enough to allow space and protection for two layers of reinforcement, so 3 to 4 in. is about as thin as any shell can be made.

c. Dome Relations, Compression Mode Loading [10]. In many problems of deformation of shells the bending stresses can be neglected, and

only the stresses due to strain in the middle surface of the shell need be considered. Under a uniform pressure action normal to the surface of the shell, the middle surface of the shell undergoes a uniform strain; and since thickness of the shell is small in relation to the other dimensions, compressive stresses can be assumed as uniformly distributed across the thickness. Usually structural arrangement is such that only vertical reactions are imposed on the dome by the supports, horizontal forces being taken by a supporting ring which undergoes a uniform circumferential extension. Since this extension is usually different from that existing in the shell, some bending of the shell will occur near the supporting ring. This bending is of a local character [10] and will be neglected.

Under the action of a uniform radial compressive force P_c, the meridional thrust is uniform throughout the shell and is given by the relation

$$T = 1/2\ R\ P_c \qquad (10.51)$$

The hoop force is also uniform throughout the dome and is given by the relation

$$H = -1/2\ R\ P_c \qquad (10.52)$$

the minus sign in equation (10.52) denoting a tensile force.

d. Dome Relations, Deflection Mode Loading. The stresses in the dome at each horizontal cross section under an antisymmetrical loading can be calculated quite accurately by applying the usual beam theory [14], using the overturning moment of the blast forces above the section under consideration and the moment of inertia of the horizontal cross section of the shell. As shown in figure 10.26, the blast loads acting

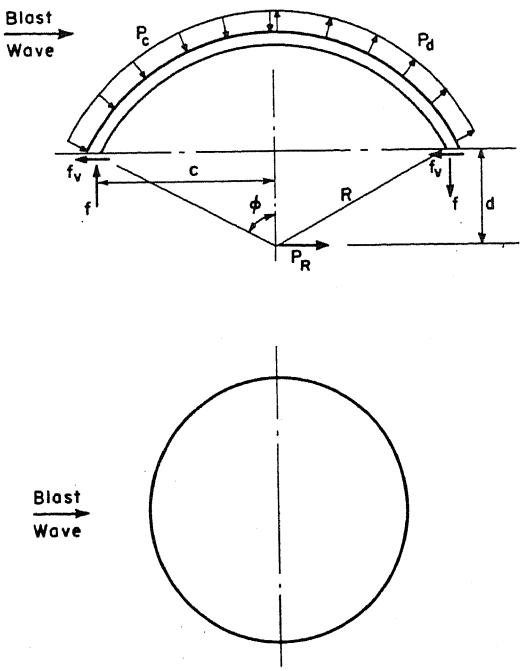

Figure 10.26. Notation for dome analysis under deflection mode loading

on the dome above any plane of latitude can be resolved into a concentrated force applied at the center of the dome in the same direction as the approaching blast wave. The necessary relations are:

$$f = \frac{Mc}{I} \tag{10.53}$$

$$f_v = \frac{P_R}{\pi R\, t} \tag{10.54}$$

where

$$M = P_R\, d \tag{10.55}$$

$$P_R = 4\, P_d R^2\, (1 - \cos \phi) \tag{10.56}$$

$$d = R \cos \phi \tag{10.57}$$

$$I = t\, R^3 \sin^3 \phi \tag{10.58}$$

and where

t = the shell thickness measured in the horizontal plane

c = the distance from the neutral axis (the neutral axis here being defined as the plane through the center of the dome, normal to the direction of the approaching blast wave)

10-15 DESIGN PROCEDURE. Step 1. Determine the size and shape of the dome, the value of the incident overpressure P_{so}, and the duration of the positive phase t_o

Step 2. Compute the overpressure-time curves, concentrating on the maximum values, by the methods of paragraph 3-19. From the calculations for several points on the dome, determine the average intensities of pressure on the windward and leeward sides of the dome. Apply equation (10.40) to these values to determine the curves of compression and deflection mode loadings.

Step 3. Assume a thickness of the dome and size of edge beam, if necessary, and the reinforcement pattern. If desired, the trial size can be obtained by a conventional design using the relations of paragraph 10-14b.

Step 4. Compute the critical radial pressure which would cause buckling of the dome of step 3 from equation (10.43). If this value of P_{cr} is less than the maximum value of the compression mode loading the thickness of the dome must be increased.

Step 5. Determine the maximum stresses due to dead weight loading and compression and deflection mode loadings for the dome of step 3 using the relations of paragraph 10-14.

Step 6. If the sum of the stresses of step 5 is less than or equal to 0.8 of the dynamic yield strength of the material, the dome is satisfactory. If these stresses are too high, the thickness must be increased until this requirement is satisfied. If the stresses are too low, the thickness of the dome should be decreased until reasonable agreement between actual and allowable stresses is achieved.

10-16 DESIGN OF A REINFORCED-CONCRETE HEMISPHERICAL DOME. To illustrate the design procedure of paragraph 10-15, a reinforced-concrete hemispherical dome is designed. The design of the footings necessary to transmit the imposed blast loads to the foundation material is not considered here as it has been covered elsewhere in this manual.

Step 1. The dome considered is a reinforced-concrete hemispherical dome of 30-ft radius. It is subjected to a maximum peak overpressure P_{so} of 10 psi, with a duration of positive phase t_o of 0.685 sec.

Step 2. Computation of load vs time curves. Since the maximum values of the compression and deflection mode loadings are of primary interest, the load vs time curves are calculated for times up to about twice the transit time t_s of the shock wave. The curves of overpressure vs time are given in figures 3.61 and 3.62 for the windward and leeward sides of the dome.

For P_{so} = 10 psi, from figure 3.9, U_o = velocity of the shock front = 1400 ft per sec; from figure 3.21, c_{refl} = velocity of sound in the reflected overpressure region = 1290 ft per sec. Therefore,

$$t_s = 2\,R/U_o = 2(30)/1400 = 0.043 \text{ sec}$$

For the windward side of the dome, the reflected overpressure is given in figure 3.11 as a function of the angle of incidence, and the drag coefficient in figures 3.68 and 3.69. The time required to clear a point on the windward side of the dome of reflection effects t_c is given by equation (3.34)

$$t_c = 3h/c_{refl} = 3(30)/1290 = 0.070 \text{ sec}$$

For the leeward side of the dome, the reflected overpressure is given by equation (3.33)

$$P_{dome} = (1.5 - \theta/180)\, P_{so}$$

and the clearing time by equation (3.34)

$$t_c = \frac{3h}{c_{refl}} \frac{\theta}{90}$$

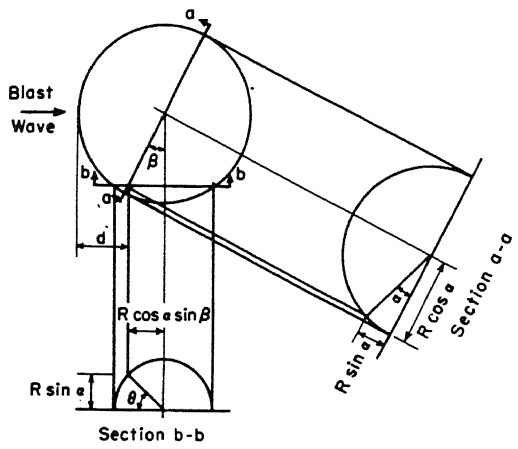

Figure 10.27. Relation between quantities used to compute blast loads

The value of overpressure for a typical point is determined as follows. Consider a value of $\beta = 22.5^{\circ}$ and a time $t = 0.115$ sec. The general shape of the load vs time curve for values of α less than 90° is given in figure 3.61. For $\alpha = 75^{\circ}$, the time required for the shock wave to reach the point being considered is given by

$$t_d = d/U_o = R(1 - \cos\alpha \sin\beta)/U_o$$
$$= 30\,[1 - (0.259)0.383]/1400$$
$$= 0.019 \text{ sec}$$

Then

$$\frac{t - t_d}{t_o} = \frac{0.115 - 0.019}{0.685} = 0.139$$

The intensity of pressure at this time, $t = 0.115$ sec, is given by the relation

$$P(t = 0.115) = P_s + C_D' q$$

where P_s, q, and C_D' are as defined in EM 1110-345-413. For $(t - t_d)/t_o = 0.139$, from table 3.1, $P_s/P_{so} = 0.750$ and $P_s = 7.50$ psi, since $P_{so} = 10.0$ psi. For $(t - t_d)/t_o = 0.139$, from table 3.2, $q/q_o = 0.530$, and $q = 1.16$ psi, since $q_o = 2.19$ psi from figure 3.24. The drag coefficient is given in figure 3.68 as a function of the angle θ. This angle is related to α and β by the relation

$$\tan \theta = \frac{R \sin}{R \cos \alpha \sin \beta} = \frac{0.966}{(0.259)(0.382)} = 9.40 \therefore \theta = 84^{\circ}$$

For $\theta = 84^{\circ}$, from figure 3.68, $C_D' = -0.90$; therefore,

$$P(t = 0.115) = 7.50 + (-0.90)\ 1.16 = 6.47 \text{ psi}$$

For those times at which the dome is subjected to reflection effects, the loads are computed as follows:

For $\alpha = 75^{\circ}$, from figure 3.11, $P_{dome} = 12.30$ psi, which is the reflected overpressure at time $t = t_d = 0.019$ sec. The clearing time is given by equation (3.34)

$$t_c = 3h/c_{refl} = (3)30/1290 = 0.070 \text{ sec}$$

Reflection effects have cleared at time $t_d + t_c = 0.089$ sec and the overpressure at this time is found to be 6.95 psi by computations similar to those above. The overpressure for any time t between $t = 0.019$ sec and $t = 0.089$ sec is found from the relation

$$P(t) = P_{dome} - \frac{t - t_d}{t_c}(P_{dome} - 6.95)$$

For $t = 0.045$ sec

$$P(t = 0.045) = 12.30 - \frac{0.045 - 0.019}{0.070}(12.30 - 6.95)$$

$$= 12.30 - 1.99 = 10.31 \text{ psi}$$

The overpressure vs time curves for times up to 0.120 sec are computed in the manner illustrated above and entered in tables 10.1 and 10.2.

The values of P_n and P_f in table 10.3 are obtained by averaging the values given in tables 10.1 and 10.2. For time $t = 0.080$ sec

$$P_n = 1/6\ (9.90 + 8.82 + 7.64 + 9.15 + 8.14 + 7.60)$$

$$= 51.25/6 = 8.54 \text{ psi}$$

$$P_f = 1/6\ (7.43 + 7.99 + 8.17 + 7.43 + 7.39 + 6.64)$$

$$= 45.05/6 = 7.51 \text{ psi}$$

Applying equation (10.40) to these values we obtain the compression and deflection mode loadings

$$P_c = 0.5\ (P_n + P_f) = 0.5\ (8.54 + 7.51) = 8.02 \text{ psi}$$

$$P_d = 0.5\ (P_n - P_f) = 0.5\ (8.54 - 7.51) = 0.52 \text{ psi}$$

Table 10.1. Overpressure vs Time Curves for $\beta = 22.5°$

Time	$\alpha = 15°$	$\alpha = 45°$	$\alpha = 75°$	$\alpha = 105°$	$\alpha = 135°$	$\alpha = 165°$
t_c =	0.070	0.070	0.070	0.075	0.083	0.088
t_d =	0.014	0.016	0.019	0.024	0.027	0.030
(sec)	(psi)	(psi)	(psi)	(psi)	(psi)	(psi)
0	0	0	0	0	0	0
0.005	0	0	0	0	0	0
0.010	0	0	0	0	0	0
0.015	17.58	0	0	0	0	0
0.020	16.99	14.80	12.22	0	0	0
0.025	16.40	14.30	11.84	9.63	0	0
0.030	15.81	13.81	11.46	9.43	9.05	8.78
0.035	15.22	13.31	11.08	9.23	8.94	8.72
0.040	14.63	12.81	10.69	9.03	8.84	8.66
0.045	14.03	12.31	10.31	8.83	8.73	8.60
0.050	13.44	11.81	9.93	8.63	8.63	8.53
0.055	12.85	11.31	9.55	8.43	8.52	8.47
0.060	12.26	10.82	9.16	8.23	8.41	8.41
0.065	11.67	10.32	8.78	8.03	8.31	8.35
0.070	11.08	9.82	8.40	7.83	8.20	8.29
0.075	10.49	9.32	8.02	7.63	8.10	8.22
0.080	9.90	8.82	7.64	7.43	7.99	8.17
0.085	9.42	8.32	7.25	7.23	7.89	8.11
0.090	9.25	8.15	6.90	7.02	7.78	8.04
0.095	9.09	8.02	6.79	6.82	7.68	7.98
0.100	8.92	7.91	6.71	6.65	7.57	7.92
0.105	8.77	7.77	6.62	6.57	7.47	7.86
0.110	8.62	7.66	6.55	6.49	7.36	7.80
0.115	8.45	7.52	6.47	6.41	7.27	7.74
0.120	8.30	7.41	6.37	6.34	7.15	7.61

Table 10.2. Overpressure vs Time Curves for $\beta = 67.5°$

Time	$\alpha = 15°$	$\alpha = 45°$	$\alpha = 75°$	$\alpha = 105°$	$\alpha = 135°$	$\alpha = 165°$
t_c =	0.070	0.070	0.070	0.081	0.102	0.119
t_d =	0.002	0.007	0.016	0.027	0.035	0.041
(sec)	(psi)	(psi)	(psi)	(psi)	(psi)	(psi)
0	0	0	0	0	0	0
0.005	23.85	0	0	0	0	0
0.010	22.77	25.91	0	0	0	0
0.015	21.70	24.59	0	0	0	0
0.020	20.62	23.27	14.07	0	0	0
0.025	19.54	21.95	13.53	0	0	0
0.030	18.46	20.63	12.99	9.12	0	0
0.035	17.39	19.32	12.45	8.95	7.72	0
0.040	16.31	18.00	11.91	8.78	7.69	0
0.045	15.23	16.68	11.37	8.61	7.65	6.51
0.050	14.15	15.36	10.83	8.44	7.61	6.53
0.055	13.07	14.03	10.29	8.28	7.57	6.55
0.060	12.00	12.72	9.75	8.11	7.54	6.57
0.065	10.90	11.40	9.21	7.94	7.50	6.59
0.070	9.71	10.09	8.68	7.77	7.47	6.61
0.075	9.30	8.77	8.23	7.60	7.43	6.63
0.080	9.15	8.14	7.60	7.43	7.39	6.64
0.085	8.98	8.02	7.06	7.27	7.36	6.66
0.090	8.81	7.89	6.87	7.10	7.32	6.68
0.095	8.66	7.76	6.78	6.93	7.28	6.70
0.100	8.52	7.64	6.70	6.76	7.25	6.72
0.105	8.35	7.53	6.62	6.59	7.21	6.74
0.110	8.20	7.40	6.54	6.47	7.18	6.76
0.115	8.06	7.28	6.45	6.39	7.14	6.78
0.120	7.90	7.17	6.36	6.32	7.10	6.80

Table 10.3. Compression and Deflection Mode Loads vs Time Curves

Time	P_n	P_f	P_c	P_d
(sec)	(psi)	(psi)	(psi)	(psi)
0	0	0	0	0
0.005	3.98	0	1.99	1.99
0.010	8.11	0	4.06	4.06
0.015	10.65	0	5.32	5.32
0.020	16.99	0	8.50	8.50
0.025	16.26	1.61	8.94	7.33
0.030	15.54	6.06	10.80	4.74
0.035	14.79	7.26	11.03	3.77
0.040	14.06	7.17	10.62	3.45
0.045	13.32	8.16	10.74	2.58
0.050	12.59	8.06	10.33	2.27
0.055	11.85	7.95	9.90	1.95
0.060	11.12	7.88	9.50	1.62
0.065	10.38	7.79	9.08	1.30
0.070	9.63	7.69	8.66	0.97
0.075	9.02	7.60	8.31	0.71
0.080	8.54	7.51	8.02	0.52
0.085	8.18	7.42	7.80	0.38
0.090	7.98	7.32	7.65	0.33
0.095	7.85	7.23	7.54	0.31
0.100	7.73	7.14	7.43	0.29
0.105	7.61	7.07	7.34	0.27
0.110	7.49	7.01	7.25	0.24
0.115	7.37	6.96	7.17	0.21
0.120	7.25	6.89	7.07	0.18

The other values of table 10.3 are computed in this manner and used to plot figure 10.28.

Tables 10.1 and 10.2 represent the load vs time curves for the indicated values of β and α. Due to the rotational symmetry of the dome, table 10.1 also represents the load curves for a β value of 157.5° and table 10.2 for a β value of 112.50°. Since these curves are for symmetrically placed points on the surface of the dome, an arithmetical averaging of these values yields the values of the average pressures on the windward P_n and leeward P_f sides of the dome. Applying equation (10.40) to

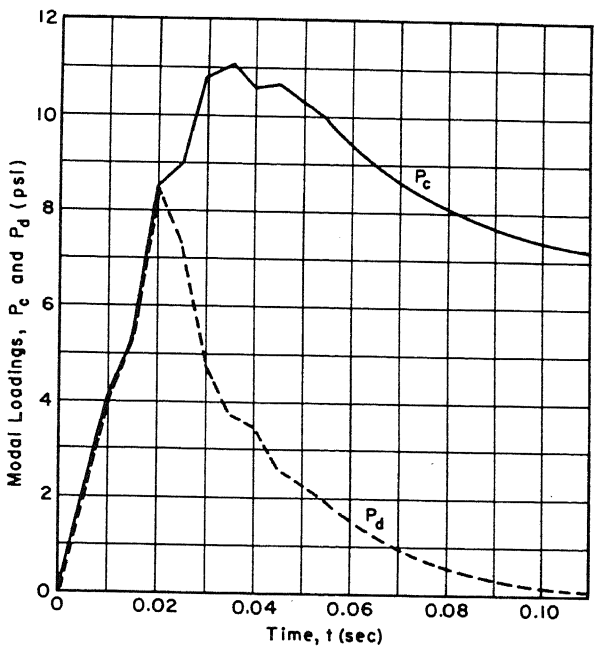

Figure 10.28. Compression and deflection mode loadings

these quantities yields the compression P_c and deflection P_d mode loadings which are plotted in figure 10.28.

Step 3. Assume a 4-in. dome thickness with a percentage of reinforcement p equal to 1.5 percent in both the meridional and latitudinal planes. Assume a modulus of elasticity E equal to 3×10^6 psi, and a dynamic concrete cylinder strength f'_{dc} equal to 3900 psi.

Step 4. From equation (10.43)

$$P_{cr} = 0.4 \frac{Eh^2}{R^2} = 0.4 \frac{3(10^6)\ 4^2}{30^2\ (144)} = 148 \text{ psi}$$

Therefore, buckling is not a problem, since the maximum compression loading pressure is 11.03 psi (table 10.3).

Step 5. The deflection mode loading produces no hoop forces in the dome as is seen from the relations of paragraph 10-14d. The compression mode loading produces meridional thrusts and hoop forces of equal magnitude over the entire dome as is seen from paragraph 10-14c. Thus, the blast forces produce meridional thrusts of greater intensity than the hoop forces and the former probably govern the design. Since the dome has equal percentages of steel in both the meridional and latitudinal directions, if the dome is strong enough to resist the meridional thrusts it is also strong enough to resist the hoop forces produced. Therefore, hoop forces are not considered in the design.

The dead load produces no ring tension along the base of the dome as is seen from equation (10.49). Since the only hoop forces produced at the base are those due to compression mode loading, the dome is capable of resisting these forces by stresses developed within the surface of the dome itself and hence, no edge beam is provided.

a. Dead Load Stresses. The unit dead weight of the dome

$$w = \frac{4}{12}\ 150 = 50 \text{ lb/ft}^2$$

Total dead load

$$W = W_u = 2\pi R^2\ w\ (1 - \cos \phi_1) \quad \text{(eq 10.45)}$$
$$= 2\pi\ 30^2\ (0.050) = 282 \text{ kips}$$

Meridional thrust at the base (maximum thrust)

$$T = \frac{W}{2\pi R \sin^2 \phi_1} \quad \text{(eq 10.47)}$$

$$= \frac{282}{2\pi\ (30)} = 1.5 \text{ kips/ft}$$

Dead load stress intensity

$$f_{dead} = \frac{1.5(1000)}{4(12)} = 31 \text{ psi}$$

b. Compression Mode Stresses. The meridional thrust is uniform over the dome, and is given by the relation

$$T = 1/2\ R\ P_c \quad \text{(eq 10.51)}$$

From figure 10.28, maximum P_c = 11.03 psi, therefore,

$$T = 1/2(30)11.03(0.144) = 23.85 \text{ kips/ft}$$

Compression mode stress intensity

$$f_{comp} = \frac{23.85(1000)}{4(12)} = 497 \text{ psi}$$

c. Deflection Mode Stresses. The bending stress is given by

$$f = Mc/I \quad \text{(eq 10.53)}$$

and the shearing stress is given by

$$f_v = P_R/\pi R\ t \quad \text{(eq 10.54)}$$

These may be reduced to

$$f = \frac{4P_d\ R\ (1 - \cos \phi_1) \cos \phi_1}{\pi h \sin \phi}$$

and

$$f_v = \frac{4P_d\ R\ (1 - \cos \phi_1) \sin \phi_1}{\pi h}$$

The resultant stress intensity is

$$f_{resultant} = \sqrt{f_v^2 + f^2}$$

and this acts at the angle θ from the vertical where

$$\theta = \tan^{-1} \frac{f_v}{f} = \tan^{-1} (\sin \phi_1 \tan \phi_1)$$

The stress intensity component in the meridional plane is given by

$$f_{defl} = \sqrt{f_v^2 + f^2} \sin (\phi_1 - \theta)$$

or

$$f_{defl} = \left[\left(\frac{4P_d R (1 - \cos \phi_1) \sin \phi_1}{\pi h}\right)^2 + \left(\frac{4P_d R (1 - \cos \phi_1) \cos \phi_1}{\pi h \sin \phi_1}\right)^2\right]^{\frac{1}{2}}$$

$$\left[\sin \phi_1 - \tan^{-1} (\sin \phi_1 \tan \phi_1)\right]$$

This may be reduced to

$$f_{defl} = \frac{4P_d R}{\pi h} \left[(1 - \cos \phi_1)^2 \left(\sin^2 \phi_1 + \cot^2 \phi_1\right)\right]^{\frac{1}{2}}$$

$$\left[\sin \left(\phi_1 - \tan^{-1} \sin \phi_1 \tan \phi_1\right)\right]$$

The maximum value of f_{defl} may be determined by trial and error and it always occurs at $\phi_1 = 39^\circ$. Thus

$$f_{defl} = \frac{4P_d R}{\pi h} (0.0644)$$

For the case at hand

$$f_{defl} = \frac{4(8.50)30(12)}{\pi 4} (0.0644) = 62.8 \text{ psi}$$

Step 6. Total of maximum stress intensities

$$f_{total} = f_{dead} + f_{comp} + f_{defl} = 31 + 497 + 63 = 591 \text{ psi}$$

Since this stress does not exceed the dynamic cylinder strength of the concrete, the shell is more than adequate to resist the applied loads. This value (591 psi) is so low that the shell thickness could be decreased. A minimum thickness of about 4 in. is necessary to provide satisfactory protection for the reinforcement, so the thickness as assumed is adopted.

BIBLIOGRAPHY

1. Timoshenko, Stephen, Vibration problems in engineering, 3rd ed., D. Van Nostrand, New York, 1955.

2. den Hartog, J. P., "Vibration of frames of electrical machines", Applied Mechanics, vol. 50, no. 17, (May-August, 1928), pp 1-5.

3. Love, Augustus E. H., A Treatise on the mathematical theory of elasticity, 4th ed., Cambridge University Press, Cambridge (Eng.), 1934.

4. Timoshenko, Stephen, and D. H. Young, Theory of structures, McGraw-Hill Book Co., inc., New York, 1945.

5. Spofford, Charles M., Theory of continuous structures and arches, McGraw-Hill Book Co., inc., New York, 1937.

6. Fife, Walter M., and J. B. Wilbur, Theory of statically indeterminate structures, McGraw-Hill Book Co., inc., New York, 1937.

7. den Hartog, J. P., "The Lowest natural frequency of circular arcs", London, Edinburgh and Dublin Philosophical Magazine and Journal of Science, Series 7, vol. 5, (1928), pp 400-408.

8. Timoshenko, Stephen, Theory of elastic stability, McGraw-Hill Book Co., inc., New York, 1936.

9. American Society of Civil Engineers, "Design of cylindrical concrete shell roofs", Manual of Standard Practice, no. 31, 1952.

10. Timoshenko, Stephen, Theory of plates and shells, McGraw-Hill Book Co., inc., New York, 1940.

11. Lundgren, Helge, Cylindrical shells, The Danish Technical Press, Copenhagen, 1951.

12. Portland Cement Association, "Design of circular domes", Concrete Information Bulletin, ST-55.

13. von Karman, Theodore and H. Tsien, "Buckling of spherical shells by external pressure", Journal of the Aeronautical Sciences, vol. 7, no. 2, (December, 1939), pp 43-50.

14. Molke, Eric C., and J. E. Kalinka, "Principles of concrete shell design", American Concrete Institute, Proceedings, vol. 34, May-June, 1938, pp 649-707.

15. Merritt, J. L., and Newmark, N. M. Design of Underground Structures to Resist Nuclear Blast. Structural Research Series No. 149, University of Illinois, April 1958.